



AD A104539

CONDITIONAL SAMPLING OF  
OCEANIC TEMPERATURE AND PRESSURE

James D. Irish

Wendell S. Brown

Mark P. Woodbury

Department of Earth Sciences  
University of New Hampshire

29 June 81

Ocean Process Analysis Laboratory  
Tech. Rept. No. 8101 -

UNH - SG-172

412552

### Acknowledgements

Many of the basic ideas behind this work evolved out of a collaborative effort begun in the early 1970's at IGPP under the direction of Walter Munk and Frank Snodgrass. The authors acknowledge the guidance provided by both of them. A prototype instrument was constructed by the Marine Systems Engineering Lab at UNH and funded by the L. Hubbard Fund. The final software development and instrument deployment was funded by the National Science Foundation grant OCE-7826229 (NSFE). The analysis was funded by the Office of Naval Research under contract N00014-80-C-0351 (HEBBLE).

*new*

*Little in file*

*A*

## INTRODUCTION

In the ocean, as in the atmosphere, energy transfer processes exhibit a distinct intermittency. Important energy transfer events occur rarely in space and time but their contribution is likely to be greater than those from all others combined. For example, the most severe storms during a particular year are likely to be associated with a larger momentum and heat flux between the atmosphere and the ocean than the winds during the rest of the year. The breaking of an internal wave can lead to a greater vertical mixing of heat and salt than other diffusion processes.

The presence of intermittency places severe demands on geophysical data acquisition. Routine sampling at fixed rates provide redundant data nearly all of the time and inadequate data during the rare times of an interesting event. A fixed program of intermittent rapid sampling superimposed on a standard low sampling rate (commonly referred to as burst sampling) is an improvement, but is not entirely satisfactory either. What is needed is a high rate of sampling conditioned by the occurrence of the rare important events or what will be referred here as conditional sampling. This is the program followed when there is strong human involvement: meteorological sampling of severe storms, oceanographic sampling of Gulf Stream rings, etc. In the ocean this kind of sampling needs to be carried out automatically. In this paper we describe how we have adapted the concept of conditional sampling to making ocean measurements.

Our particular focus is on sea floor pressure and temperature fluctuations, which exhibit intermittent behavior in relation to different types of oceanic events. The detection of potentially destructive waves such as tsunamis, storm surges and solitary waves would be possible with a bottom pressure sensor if it were sampling at the appropriate rate. The temperature signature of an internal bore or breaking internal wave would go undetected or be severely undersampled with a two-hour sampling scheme which might normally be employed for long term deployments.

The thrust of recent University of New Hampshire (UNH) work is the study of continental shelf circulation with arrays of bottom temperature and pressure instruments. In the near future we plan to deploy temperature/conductivity chains above the bottom pressure instrument for purposes of measuring the baroclinic and barotropic contributions to the pressure gradient field. The addition of a conditional sampling scheme to this instrumentation will permit us for the first time to resolve the important intermittent events which affect the local shelf circulation processes. By doing so we will be able to study the relative importance of internal waves, internal bores, upwelling and other turbulent processes in the redistribution of mass, heat and momentum.

This report discusses our preliminary efforts to conditionally sample bottom pressure and temperature with prototype instrumentation. For this work we sample the low frequency energy in the bottom pressure and temperature field with a standard UNH P/T recorder we have named KELVIN. The recording of high frequency fluctuations is controlled by a microprocessor-based conditional sampling unit we call COSAP. In the following sections we discuss this instrumentation in terms of (a) the definition of conditional sampling and a proposed solution, (b) a hardware description and (c) some preliminary field results and conclusions.

#### DEFINITION AND SOLUTION OF THE SAMPLING PROBLEM

We use the term CONDITIONAL SAMPLING to refer to the preprocessing of data, variable sampling rate for different sensors, temporary storage of past data, error detection, event detection and final data storage. Each of these features is discussed below in detail.

1) PREPROCESSING. Before being recorded, some preprocessing of the incoming signals is usually required. For example, the averaging done by counting the sensor frequency over the sample interval is usually adequate to suppress

high frequency fluctuations and reduce aliasing. Another example is the vector averaging of current meter speed and direction observations. Other preprocessing might include the calculation of the mean or variance of the incoming observations. Derived quantities such as Reynolds stress and sediment transport can be computed insitu from the cross-correlations between appropriate sensors.

2) ERROR DETECTION AND NOISE REDUCTION. Spurious values may be encountered when the equipment is being launched or due to sensor or cable failure. Regardless of the cause, it is desirable to eliminate these spurious data before any event detection calculations are performed on the data. It would be frustrating to have a detailed record of a sensor failure in the place of real data. We employ a simple error detector based on a first difference approach to sense "spurious" data. Geophysical signals are generally known well enough so that spurious first differences can be specified (i.e. five times the maximum expected first difference), so that the corresponding spurious data can be identified and discarded.

3) PAST DATA STORAGE. In order to save observations associated with the onset of an event, an intermediate data storage area is required. In our application, the the past 128 samples (or 2 hours 16 minutes 32 seconds) of temperature and pressure values are temporarily stored.

4) EVENT DIRECTION. The simplest form of event detection initiates data storage when the signal exceeds a preset level. If past data values have been stored then they can be recorded along with subsequent data from the event. A higher order detection scheme uses the variance level (rather than the signal itself) to initiate data storage. Still further, digital filtering can be performed on the data to suppress the tides and other low frequency energy which dominate the record. We employ the latter scheme which uses the energy level in a selected frequency band (referred to as an event window) to initiate data storage.

5) VARIABLE SAMPLING. Modification of particular sampling programs are relatively easy to incorporate since we use microprocessor-based data loggers. For example, selected sample rates and adaptive sampling are to be considered in future versions of UNH instrumentation.

(a) Selected Sample Rates. With conventional recording systems, all sensors are usually sampled at the same rate. With a microprocessor-based recording system, it becomes much easier to select the sample rate for each sensor, based on a knowledge of the sensor response and behavior, and on the geophysical processes to be measured. For our solution discussed below, we still sample all sensors at the same rate.

(b) Adaptive Sampling: This feature permits the microprocessor to change the original sampling scheme as the experiment progresses. By monitoring the number and duration of events as well as the time and amount of data storage remaining in the experiment, the event detection parameters can be adjusted to optimize the use of the tape capacity available for the duration of the experiment.

#### CONDITIONAL SAMPLING - A SPECIFIC SOLUTION

We present a scheme for resolving high frequency seafloor pressure and temperature fluctuations with prototype instrumentation which has been tested in the coastal waters of New England. In addition, we briefly discuss planned improvements in the present form of the instrumentation and sampling scheme. A block diagram of our prototype system is shown in Figure 1 and discussed below.

The sampling theorem tells us that a sample interval  $\Delta$  resolves frequencies up to the Nyquist frequency ( $f_N = (2\Delta)^{-1}$ ). Thus our routine low frequency sample interval of 1 hour, resolves frequencies up to 0.5 cph which is adequate for tides and lower frequency fluctuations. However, intermittent

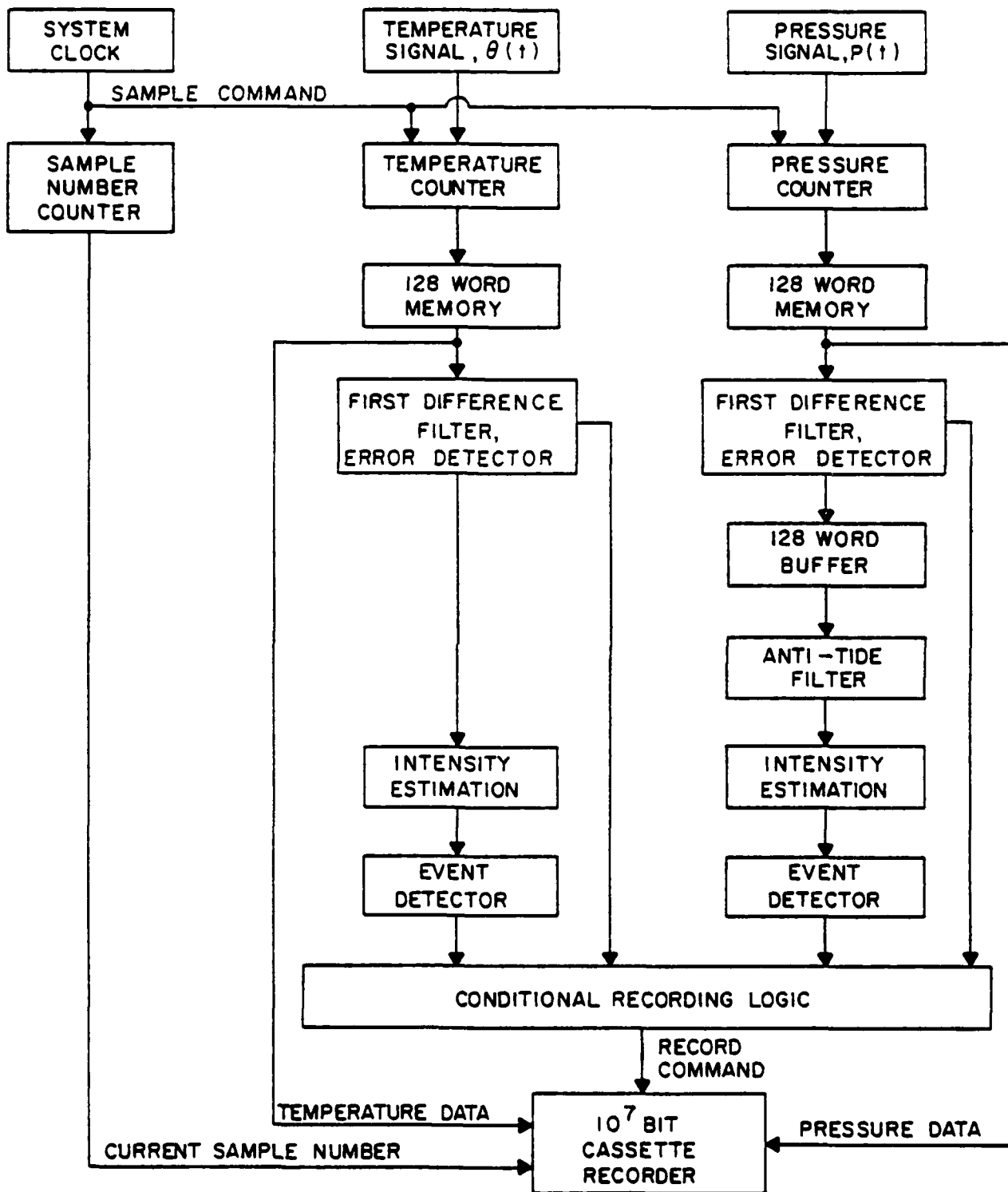


Figure 1. A block diagram showing the flow of data through the conditional sampling process.

events with higher frequency energy, such as mixing events or tsunamis, contain significant fluctuations at periods between one hour and one minute. We use a conditional sampling scheme to sample these high frequency processes at one minute (actually 64 seconds) intervals when they occur. A one minute sample interval was chosen since it is the high frequency cut-off due to attenuation of surface waves with depth in the deep ocean (5000 m). Thus the "event window" as defined here covers the range of frequencies from 0.5 cph to 28 cph.

#### ROUTINE LOW FREQUENCY SAMPLING

A low frequency sample is currently processed by standard Sea Data electronics which average the temperature and pressure sensor outputs over the sample interval to 24 bit resolution. For a 4 year experiment, the 10 megabit cassette permits us to sample at a period of 30 minutes if we wish. Thus frequencies up to the Nyquist of 1 cph can be resolved.

The same temperature sensor is interrogated at both the *high and low* frequency sample rate and is a quartz thermometer with a nominal sensitivity of 1000 Hz/°C. The pressure sensor is also a quartz instrument with a sensitivity around 13 Hz/dbar. A record, consisting of a sample number, temperature count, pressure count, parity and a record gap, is written on cassette tape every sample interval.

#### CONDITIONAL HIGH FREQUENCY SAMPLING

A high frequency sample consists of a 64 second average of temperature and pressure which is temporarily stored in the microprocessor-memory to 12-bit accuracy. For this averaging interval the temperature sensor has a least count resolution of 15  $\mu$ °C, and a 12-bit counter overflows every 0.064°C. The resolution is too great, and the overflow too frequent, so the sensor frequency was divided by 8 to give a least count of 1/8 m°C, and a counter

overflow of 1/2°C. For this averaging interval the pressure sensor has a least count of 0.12 mbars (cm of sea water) and the 12 bit counter overflows every 5dbars. Since we can obtain the most significant temperature and pressure bits from either the non-event sample or with the acoustic system described below, the above resolutions and overflows are acceptable.

The spectral noise due to the digitizing interval or least count, LCN, is

$$LCN(f) = \frac{(LC)^2}{6 f_N} [1 - \cos(2\pi\Delta f)] \quad , \quad (1)$$

where the least count,  $LC = 1.2 \times 10^{-3}$  dbars, the Nyquist frequency  $f_N = 28.125$  cph and the sample interval  $\Delta = 64$  seconds. This is more than a decade below the expected signal level at the Nyquist frequency, so the effects of the quantization of the geophysical signal can be neglected in this case.

The fm-signal from each sensor is counted over the 64-second sample interval; a process which suppresses high frequency fluctuations. The equivalent filter response of the averaging process,  $H_e(f)$ , is

$$H_e(f) = \frac{\sin(\pi f \Delta)}{\pi f \Delta} \quad . \quad (2)$$

At the Nyquist frequency the filter is down 4 db and the envelope of the side-lobes decreases as  $f^{-2}$ .

The 12-bit temperature and pressure samples are stored sequentially in Random Access Memory (RAM) and a sample counter is incremented each sample. After the 128-sample buffer is full and the conditions for recording data (described in detail below) are met, 24 bits of diagnostics, 24 bits of the current sample number and 3072 bits of data are written into one file containing two records on a cassette tape. Subsequent data samples replace the oldest data in RAM, one sample at a time for at least 128 samples and then thereafter until a record command is received again. In future instruments, we will eliminate the separate low frequency recording hardware and then the micro-

processor will control the storage of both low frequency and high frequency data.

#### FIRST DIFFERENCING AND ERROR DETECTION

The first step in the conditional decision making scheme is the first differencing of the raw data. Since most geophysical spectra decrease with increasing frequency (red spectra), the first difference filter suppresses low frequency variations such as drift and acts as a data prewhitener.

To screen the data for errors, each first difference is compared with a preset level,  $B_p$ , which is larger than the first difference expected from geophysical signals and yet small enough to eliminate spikes associated with instrument malfunction. Specifically the first difference for pressure,  $p'$ , is computed according to

$$p'(t) = \begin{cases} p(t) - p(t-1) & \text{if } p'(t) \leq B_p \\ p'(t-1) & \text{if } p'(t) > B_p \end{cases} \quad (3)$$

To obtain the response of this first differencing filter, we write

$$p'(t) = \int p(t-\tau) w(\tau) d\tau, \quad (4)$$

where the  $w(\tau)$  are the set of convolution weights

$$w(\tau) = \delta(\tau) - \delta(\tau-\Delta) \quad (5)$$

and  $\Delta$  is the 64 second sample period. By the convolution theorem, the spectrum of a first differenced record is the product of the record spectrum and the convolution weight spectrum which is found by first Fourier transforming the weights according to

$$W(f) = \int_{-\infty}^{\infty} w(\tau) e^{-2\pi i f \tau} d\tau = 1 - e^{2\pi i f \Delta} \quad (6)$$

The spectral response shown in figure 2 is then

$$WW^* = (1 - e^{2\pi i f \Delta})(1 - e^{-2\pi i f \Delta}) = 4 \sin^2(\pi f \Delta), \quad (7)$$

where \* denotes the complex conjugate. The phase lag of the filter is given by

$$\phi = \tan^{-1} \left[ \frac{\sin 2\pi f \Delta}{1 - \cos 2\pi f \Delta} \right] = [\pi/2 - \pi f \Delta] \quad (8)$$

and is also shown in figure 2. The significant phase changes, in our frequency band of interest do not affect our results since only the signal magnitudes are used for detection.

Anticipating further tide filtering the pressure first differences are stored in a "press down" 128 sample stack so the newest value is always available first. Since temperatures are not tide-filtered, a stack is not required and only the current first difference value is stored.

#### ANTI-TIDE FILTER

The principal variance in the bottom pressure signal is due to tidal oscillations. In order to see the higher frequency variations we remove tidal effects with, a digital filter which is applied to the first differenced pressure data. To construct this filter, consider the weighted sum

$$p'(t) + \alpha_1 p'(t-\delta) + \beta_1 p'(t-2\delta) = \int p'(t-\tau) W_1(\tau) d\tau \quad (9)$$

where  $W_1(\tau) = 1 + \alpha_1 \delta(\tau-\Delta') + \beta_1 \delta(\tau-2\Delta')$  and  $W_1$  and  $\Delta'$  are not related to the  $W$  and  $\Delta$  above and  $\Delta'$  is an arbitrary lag chosen with  $\alpha_1$  and  $\beta_1$  to remove the diurnal tides. Similarly define  $W_2$ ,  $\alpha_2$  and  $\beta_2$  to remove the semidiurnal tides. By the convolution theorem, the response of the combined filters is

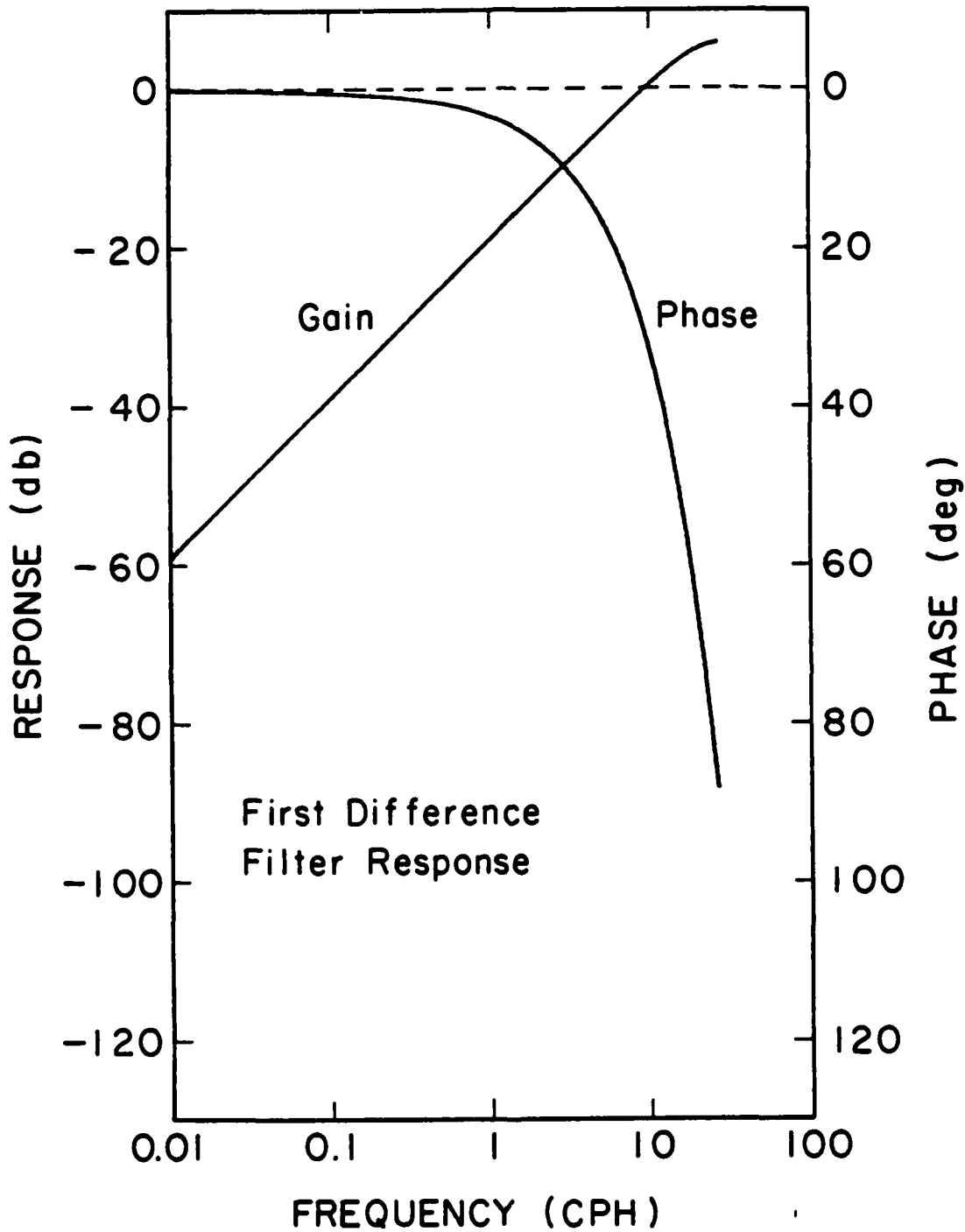


Figure 2. The amplitude response (in db) and the phase response (in degrees) of the first differencing filter.

$$\begin{aligned}
 W(f) &= W_1(f) W_2(f) \\
 &= (1 + \alpha_1 Z^{-1} + \beta_1 Z^{-2})(1 + \alpha_2 Z^{-1} + \beta_2 Z^{-2}), \quad (10)
 \end{aligned}$$

where  $Z \equiv \exp(2\pi if\Delta')$ . Multiplying and collecting terms leads to

$$\begin{aligned}
 W(f) &= 1 + (\alpha_1 + \alpha_2) Z^{-1} + (\alpha_1\alpha_2 + \beta_1 + \beta_2) Z^{-2} \\
 &\quad + (\alpha_1\beta_2 + \alpha_2\beta_1) Z^{-3} + \beta_1\beta_2 Z^{-4}, \quad (11)
 \end{aligned}$$

which when transformed back into the time domain becomes

$$\begin{aligned}
 w(\tau) &= \delta(\tau) + (\alpha_1 + \alpha_2) \delta(\tau - \Delta') + (\alpha_1\alpha_2 + \beta_1 + \beta_2) \delta(\tau - 2\Delta') \\
 &\quad + (\alpha_1\beta_2 + \alpha_2\beta_1) \delta(\tau - 3\Delta') + \beta_1\beta_2 \delta(\tau - 4\Delta'). \quad (12)
 \end{aligned}$$

We choose a lag interval,  $\Delta'$ , of 30 samples (30 samples at 64-second intervals equals 32 minutes) so that the combined filter requires inputs from the previous  $4\Delta'$  or 120 samples (2 hours 8 minutes). In practice these inputs are obtained from our temporary 128 first difference "press down" stack.

To determine the weights, appropriate for this filter consider the diurnal spectral response

$$W_1(f) W_1(f)^* = 1 + \alpha_1^2 + \beta_1^2 + 2\alpha_1(1 + \beta_1) \cos(2\pi f\Delta') + 2\beta_1 \cos(4\pi f\Delta') \quad (13)$$

where  $\Delta' = 30$  samples (32 minutes). The diurnal tidal energy is concentrated in the two tidal lines  $O_1$  and  $K_1$  with frequencies 0.03861637 cph and 0.04178074 cph respectively. We have chosen the mean frequency as appropriate for the diurnal tides, which yields  $f_1 = 0.040255$  cph. This permits one to compute  $\alpha_1$  in accordance with

$$\alpha_1 = -2 \cos(2\pi f_1 \Delta') = -1.9818307 \text{ and } \beta_1 = 1.0 \quad (14)$$

Thus the spectral response of the diurnal filter,

$$W_1 W_1^* = 16 \sin^2 [\pi(f+f_1)\Delta'] \sin^2 [\pi(f-f_1)\Delta'], \quad (15)$$

has a notch at  $f = f_1$  as shown in figure 3.

Similarly, the semidiurnal tides have their principal energy at the  $M_2$  and  $S_2$  lines, with frequencies 0.0805114 cph and 0.0833333 cph with most of the energy concentrated in the  $M_2$  line. Taking  $f_2 = 0.08051$  cph, choose  $\alpha_2 = -2 \cos(2\pi f_2 \Delta')$  = -1.927653 and  $\beta_2 = 1.0$ , leads to the corresponding semidiurnal response as shown in figure 3.

The individual sections of the tide filter have suppression greater than 110 db in the two tidal bands. The behavior of the filter would be improved by broadening the notch. This can be accomplished by letting round-off error in the computation cause the notch to "jitter".

The combined filter weights are

$$\begin{aligned}
 w(0\Delta) &= \alpha_0 &= 1.0 \\
 w(30\Delta) &= \alpha_1 + \alpha_2 &= -3.909481 \\
 w(60\Delta) &= \alpha_1 \alpha_2 + \beta_1 + \beta_2 &= 5.820277 \\
 w(90\Delta) &= \alpha_1 \beta_2 + \alpha_2 \beta_1 &= -3.909481 \\
 w(120\Delta) &= \beta_1 \beta_2 &= 1.0
 \end{aligned}
 \tag{16}$$

The spectral response of the composite tide filter is shown in figure 4. The low frequency and tidal frequency signals are attenuated 80 db. and by more than 100 db. respectively.

To further examine the suppression of the tide filter, consider the  $S_2$  tidal line which is separated from  $f_2$ , by 0.00282 cph. This line will leak the most energy into the tide-filtered pressure series. Energy at the  $S_2$  frequency is suppressed 70 db by the tide filter, and 41 db by the first difference filter for a total of 111 db. Before any filtering, a 1m amplitude  $S_2$  tide is 60 db above a 1mm wave at 1 cph. After first difference and tide filtering, the  $S_2$  signal is reduced to 32 db below the 1 cph wave. Additionally the ocean itself attenuates the pressure signature frequency (short wavelength) surface waves in

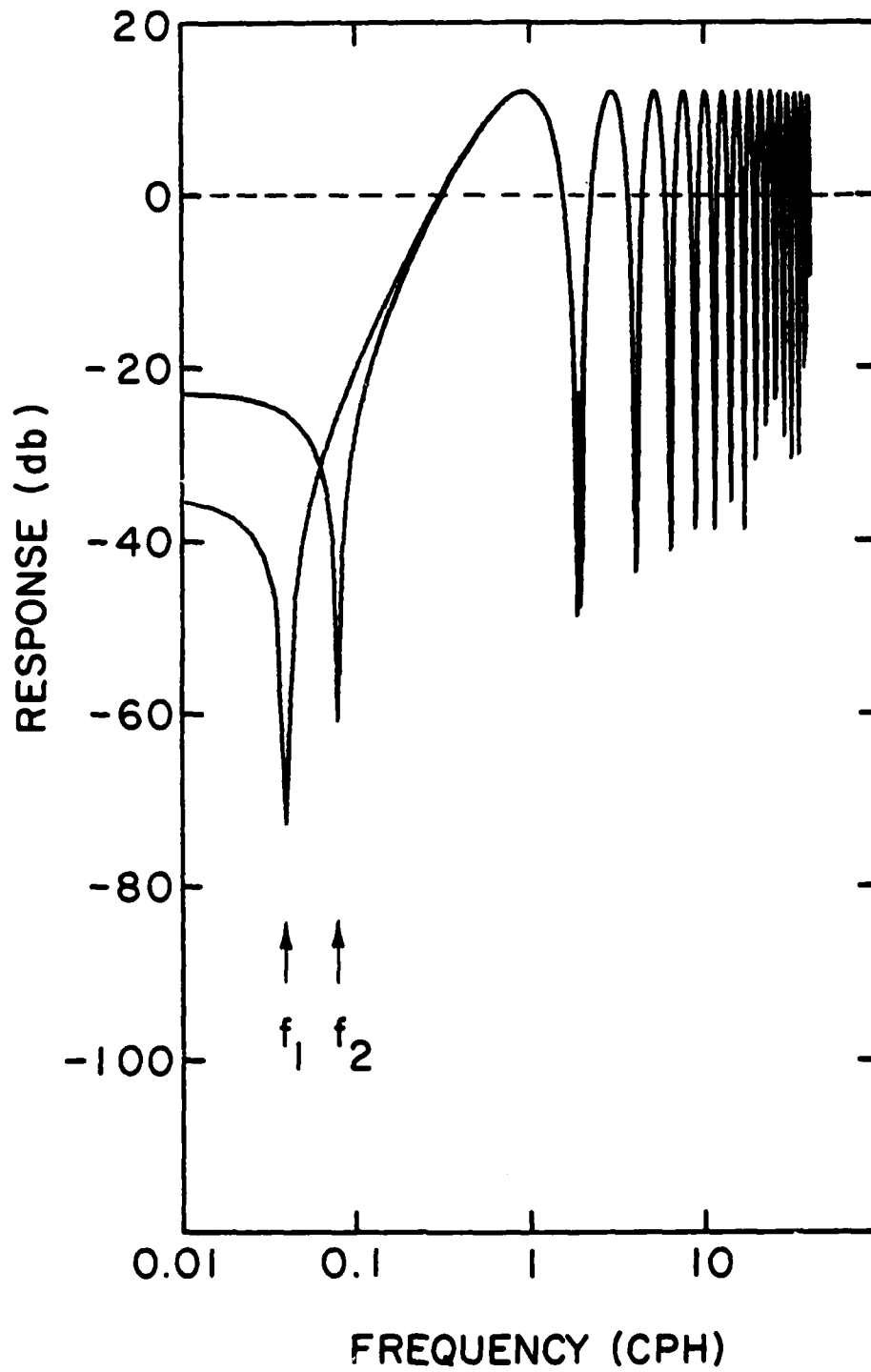


Figure 3. The response of the "idealized" diurnal and semidiurnal notch filters to eliminate tidal variations.

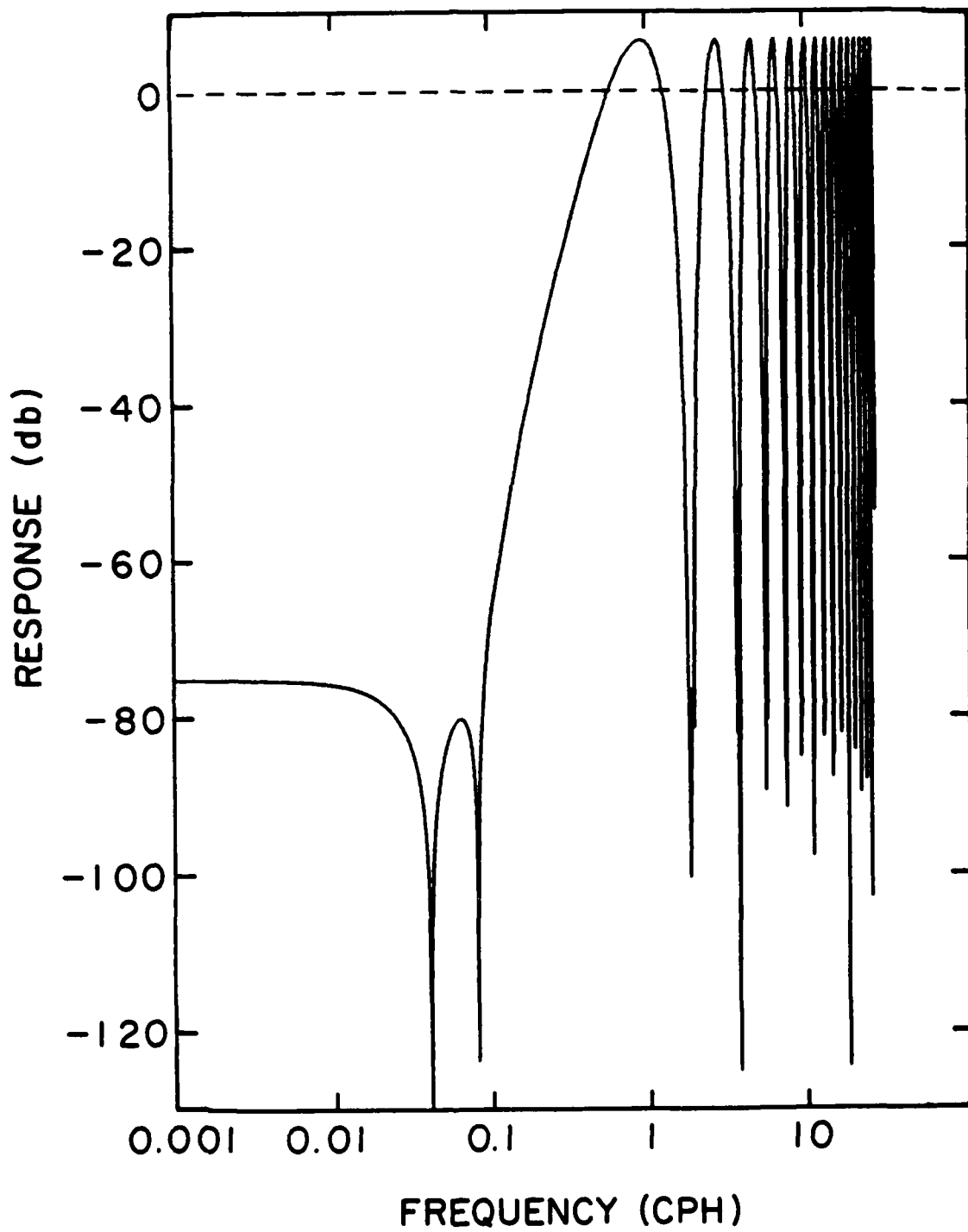


Figure 4. The response of the "anti-tide" filter defined by the weights listed in equation 16.

the bottom pressure signal. The amplitude of surface gravity waves is attenuated by the factor  $2[\cosh(KH)]^{-1}$ , where H is the depth of water, and K the wavenumber ( $2\pi/\text{wavelength}$ ) of the variation. Since the wave frequency wave is related to the wavenumber and water depth according to

$$\omega^2 = gK \text{TANH} (KH) \quad (17)$$

the high frequency cutoff for surface waves will decrease with increased depth. This bottom pressure attenuation is plotted in figure 5 for a 200m shelf and a 5000m open ocean. For the shelf the attenuation effect is negligible out to the 28 cph Nyquist frequency for our sampling. However, in the deep ocean the filtering effect is important for waves above 30 cph and it makes no sense to sample pressure at a higher rate.

At this stage of data processing the pressure data have been altered by the combined effects of the four filtering operations described thus far. We call the product of these filters the "event window". A plot of the separate filter components is shown in figure 6, and the resulting "event windows" for temperature and pressure are shown in figure 7.

One must consider how the "event window" will affect real signals before adequate event triggers can be chosen. We do so by considering the results from a test on the New England shelf. The spectra of the pressure record and the first differenced pressures are shown in figure 8. The first difference spectrum is nearly white with the tides superimposed. The spectrum of the event windowed signal (which includes tide filtering) is shown as the shaded region in figure 8. The event window in this case covers frequencies from 0.5 to 28 cph and nicely complements the frequency coverage of the low frequency recorder.

The temperature signal is first-differenced but not tide filtered so the temperature and pressure event windows differ as discussed previously. A smoothed bottom temperature spectrum is shown in figure 9 with the various

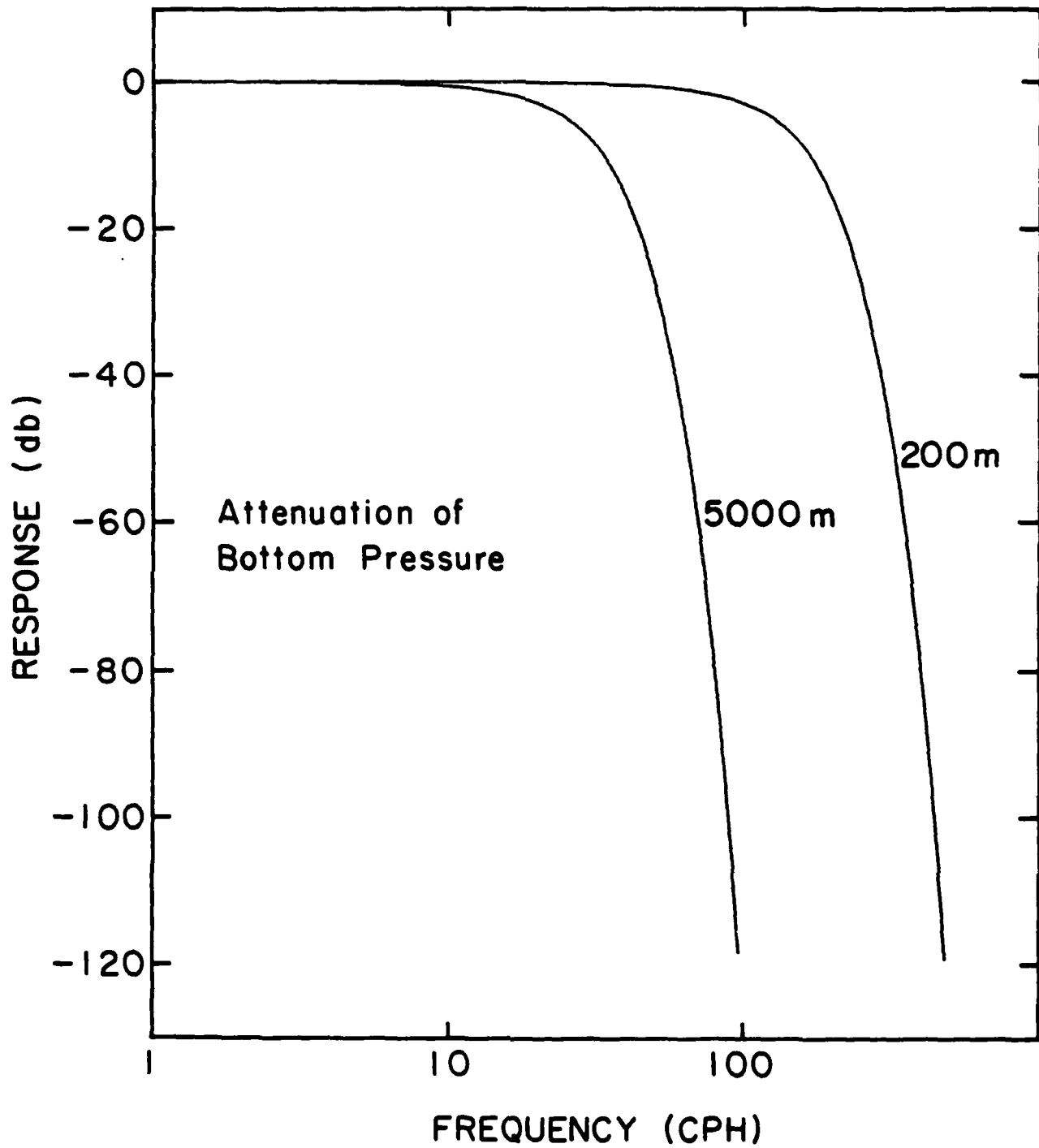


Figure 5. The attenuation of pressure with frequency is shown at two depths representative of the deep shelf and open ocean.

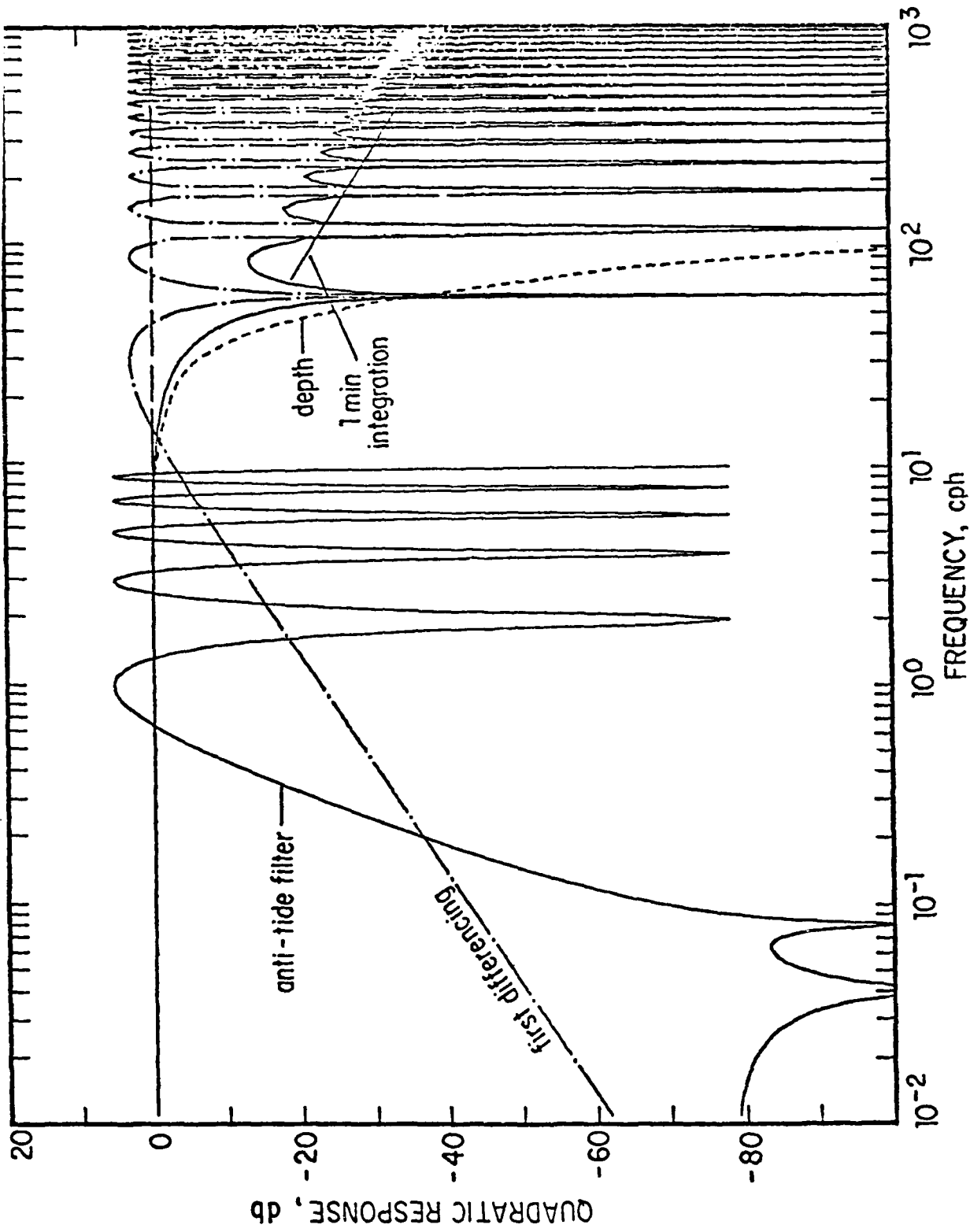


Figure 6. The various components of the actual data window (the sum of filters applied) are shown.

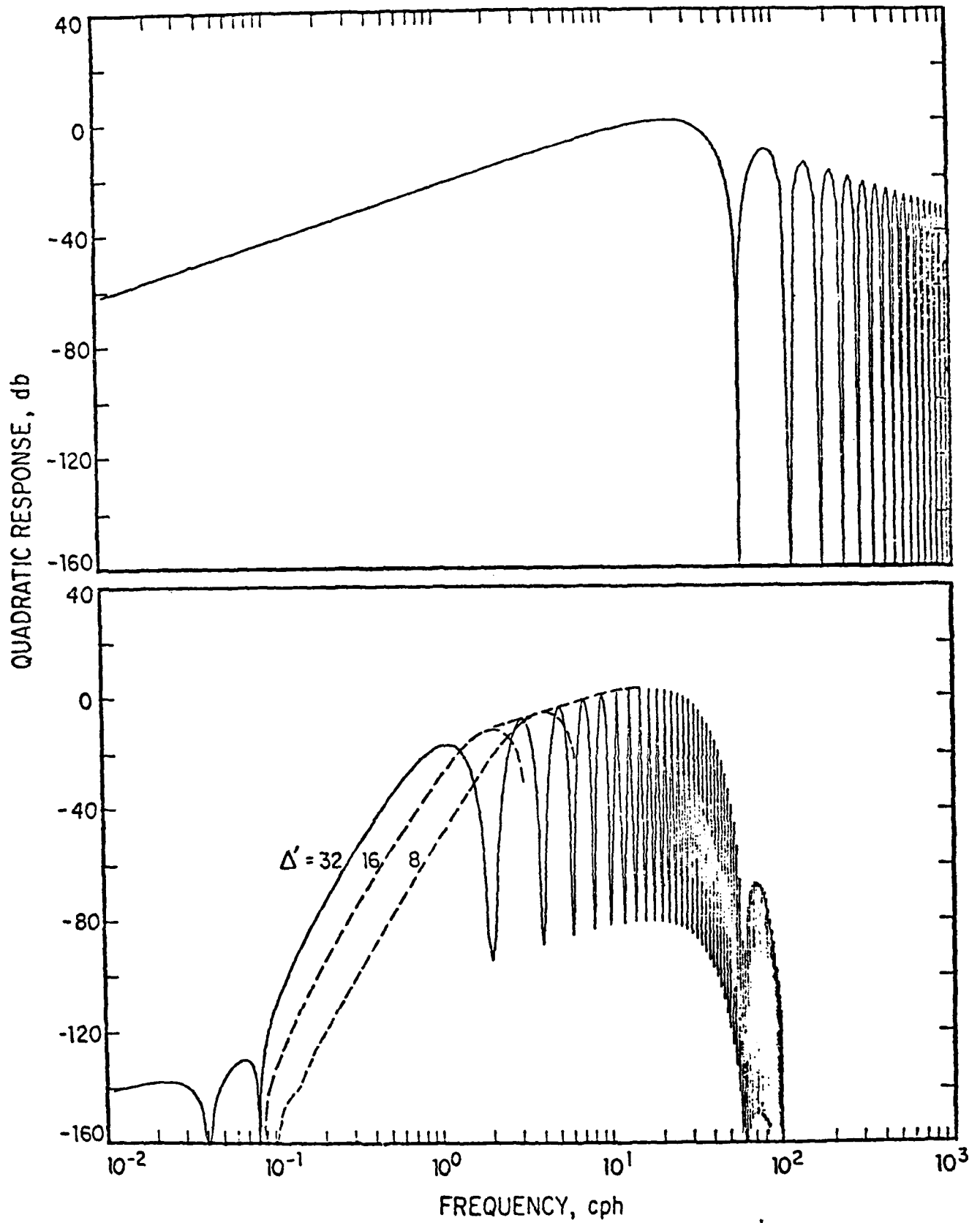


Figure 7. The temperature and pressure data windows.

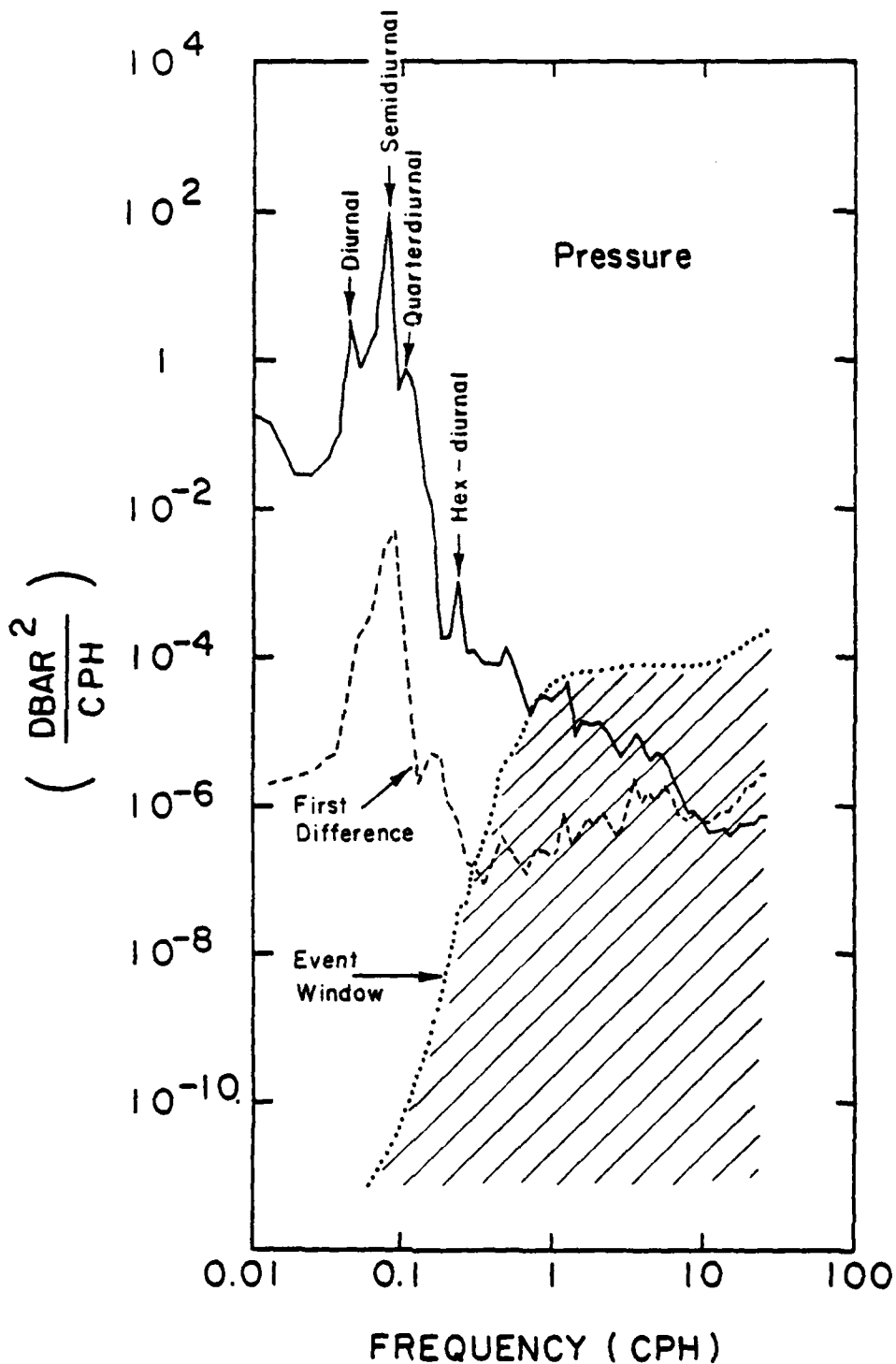


Figure 8. A shelf pressure spectrum from the test shown in Figure 15. Also shown are the first differenced spectrum and the data window, which is the shaded region defined by the spectrum of the tide filtered data.

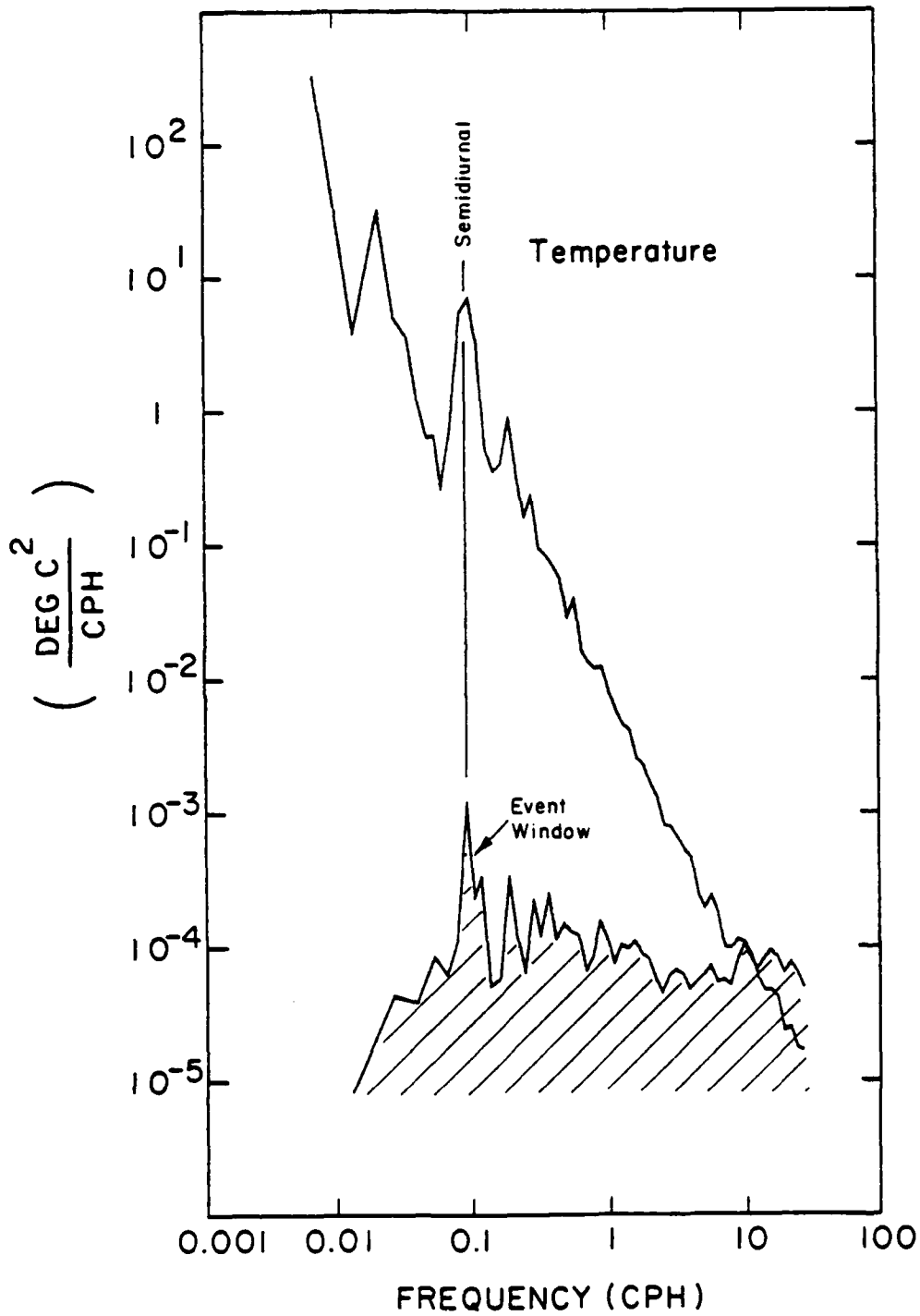


Figure 9. A shelf temperature spectrum from the test shown in Figure 15. The data window (defined by the spectrum of the first differenced record) is shaded. Note that the record is dominated by the tidal peak.

filter effects shown. The final event windowed signal on which the event detector works has a nearly white spectrum with tides superimposed. In this case the most energetic signal is at tidal frequencies and will dominate the event detection. Therefore, some high pass filtering might be incorporated if the detection of higher frequency temperature events is of interest.

#### INTENSITY CALCULATION

The actual event detection is triggered when the intensity of the event windowed signal exceeds a preset "critical" level. The temperature and pressure intensity are computed from the first differenced temperature,  $\theta'_t$ , and first differenced tide-filtered pressure,  $p''_t$ , respectively. Specifically for pressure, the intensity,  $\tilde{p}_t$ , is defined as

$$\tilde{p}_t = \gamma \tilde{p}_{t-1} + (1-\gamma) |p''_t| \quad , \quad (18)$$

where  $\gamma = 0.9835$  in an exponential fading with a time constant = 60 samples (64 minutes) and is a weighted sum of past and present values.

To examine this intensity calculation further, consider several examples with reference to figure 10.

- a). In figure 10a the temperature record,  $\theta$ , has a step change of  $\Delta\theta = 100$  counts at  $t_0$  with a corresponding first difference value at  $t_0$  of 100. The intensity,  $\tilde{\theta}$ , has only this input at  $t_0$  and therefore decays from its maximum value of  $0.0165 \Delta\theta$  as time increases.
- b) As shown in figure 10b the pressure record,  $p$ , also has a step change of  $\Delta p = 100$  counts at  $t_0$ . As seen in the lowest panel a pressure step of the same magnitude as temperature produces a larger intensity which lags the step. The first difference filter produces the series  $p'$ , consisting of a spike with an amplitude of 100 at  $t_0$ . As time increases, the anti-tide filter produces a series of 5 spikes,  $p''$  with

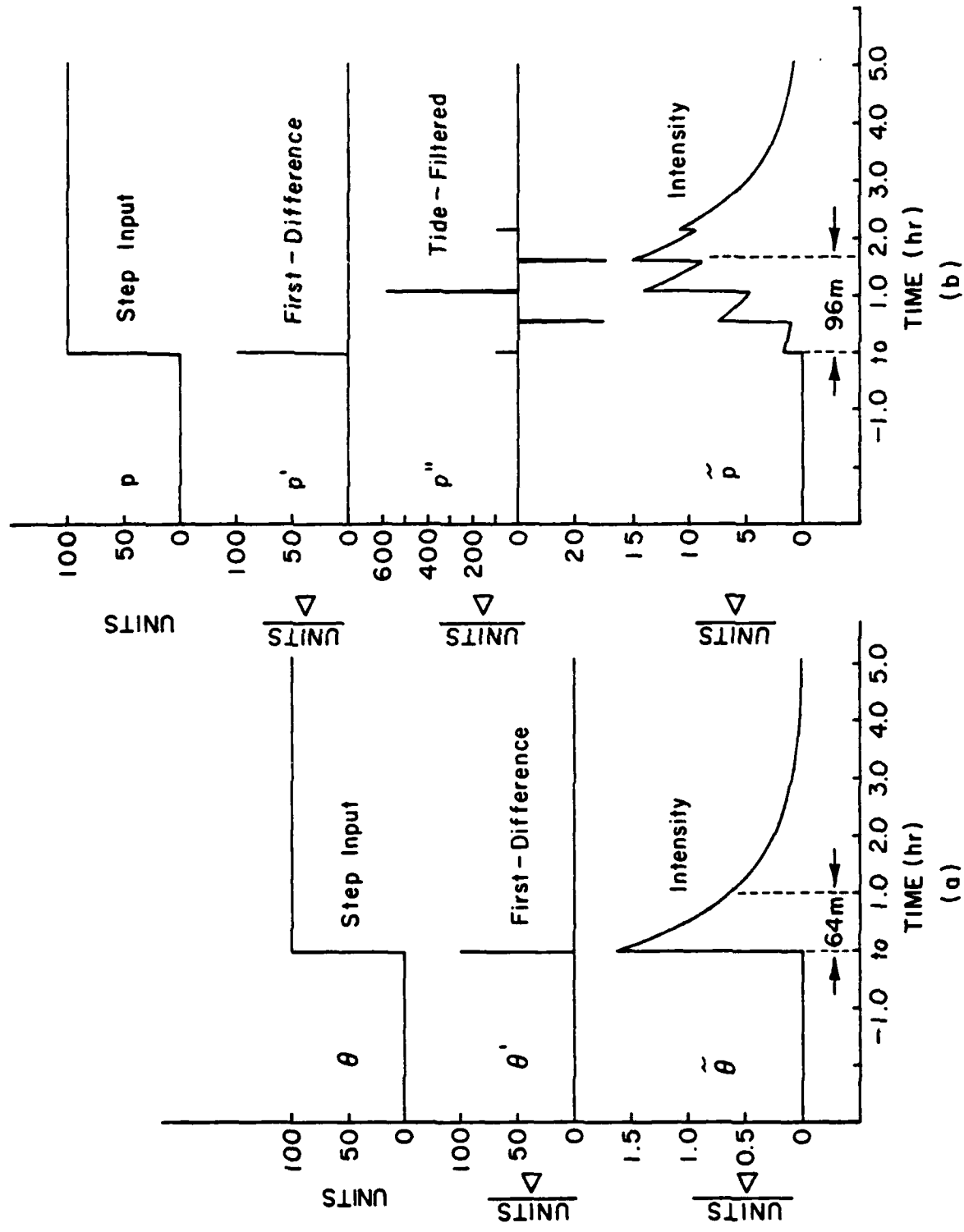


Figure 10. Examples of the response of the temperature filter (a) and pressure filter (b) to a step change in input. See text for discussion.

amplitudes of the weights  $W$  times 100 (100, -391, 582, -391, 100) at lags of 0, 30, 60, 90 and 120 samples respectively. The intensity,  $\tilde{p}$ , now a more complicated function, reaches its maximum of  $0.1503 \times \Delta p$  96 minutes after  $t_0$ . The series,  $p$ ,  $p'$ ,  $p''$  and  $\tilde{p}$  are shown in figure 10b for comparison.

The sudden onset of a wave is modeled in figure 11 by turning on a sine wave with a 100 count amplitude at  $t_0$ . The intensity takes about 5 hours to build up to its asymptotic value. Thus the intensity calculation will take some 5 hours to equilibrate to the environment at the beginning of an experiment.

#### EVENT IDENTIFIER AND RECORDING

An event is identified when the intensity,  $\tilde{p}$  or  $\tilde{\theta}$ , exceeds the appropriate preselected "critical" values,  $D_p$  or  $D_\theta$ . An intelligent choice of  $D_p$  and  $D_\theta$  depends on some knowledge of the environmental energy levels to be encountered. The  $D$ 's should be low enough so that geophysical events of interest are not missed and yet great enough so that the occasional sensor malfunction, which goes uncorrected by the first difference spurious data gate, does not trigger an event.

The spurious data gate is designed to eliminate any first difference (data spike) exceeding some preselected value ( $B_p$  or  $B_\theta$ ). A series of smaller spikes, which are not removed by this detector, could occur in a short time, accumulate and be equivalent to a single large spike. For example, if  $n$  spikes with amplitudes of nearly  $B_p$  or  $B_\theta$  occur in a short time they will be equivalent to a single spike of amplitude  $nB_p$  or  $nB_\theta$ . A single spike of amplitude  $nB_\theta$  in the temperature record will show up as two spikes of amplitude  $nB_\theta$  and  $-nB_\theta$  in the first difference record. The intensity will then see a boost equal to  $2. \times 0.0165 \times nB_\theta$ . Therefore a reasonable relationship between the "critical" level and spikes becomes

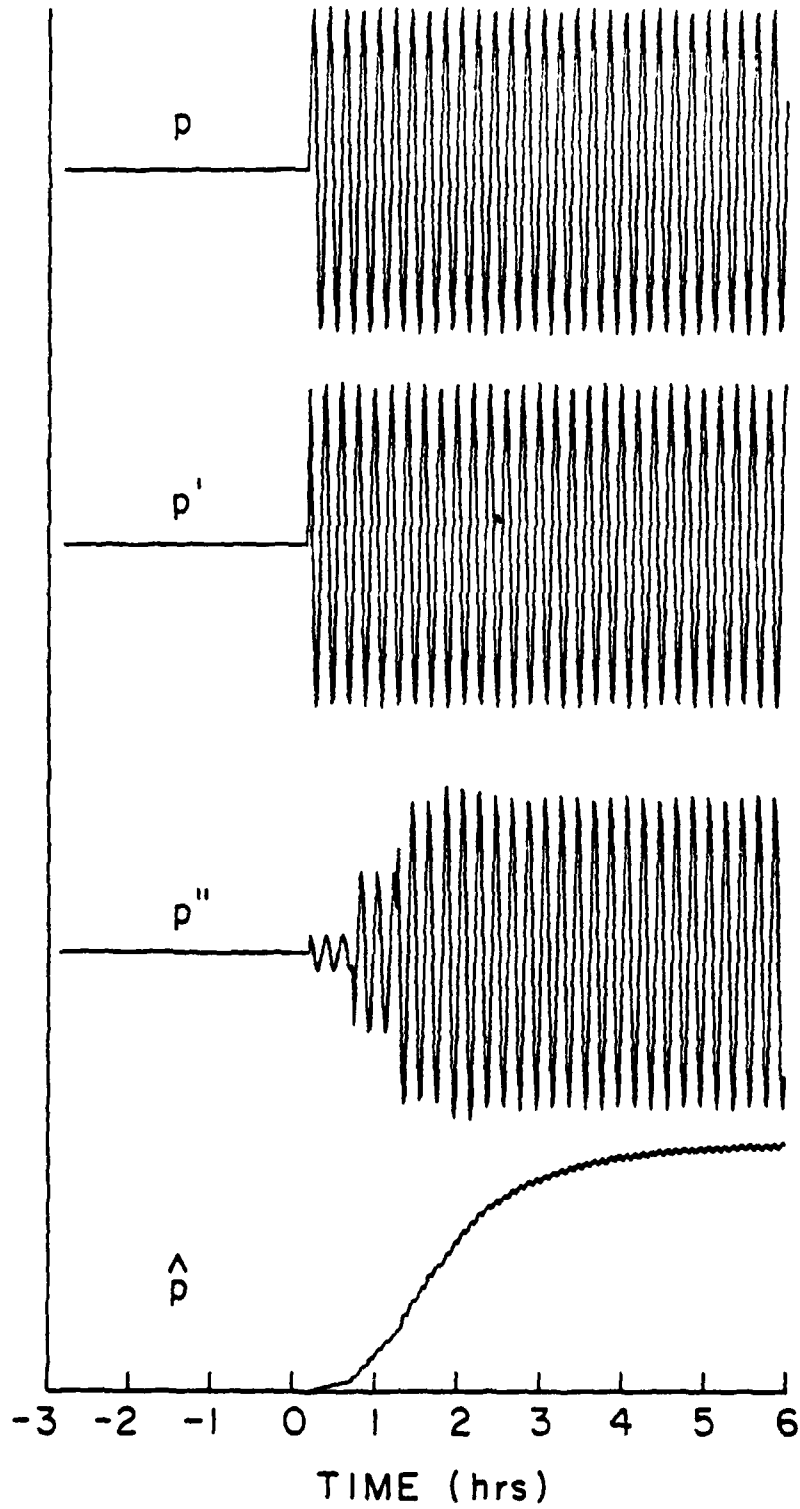


Figure 11. Examples of response to a gated burst in pressure showing the time constant of the intensity calculation.

$$D_{\theta} > 0.033 nB_{\theta} .$$

Similarly for pressure, a spike in the pressure has twice the effect of a step, and we must set  $B_p$  so that the corresponding relation is

$$D_p > 0.301 nB_p . \quad (19)$$

For our scheme we have chosen  $n = 4$  so that the appropriate conditions for choosing "critical" levels become

$$D_{\theta} > 0.132 B_{\theta} \quad (20)$$

and

$$D_{\phi} > 1.20 B_p . \quad (21)$$

Presumably these levels will not permit triggering due to spurious data input.

Once the B and D levels are chosen we require that the following criteria be satisfied for either a temperature or pressure critical to cause the data in the 128 sample buffer to be recorded.

- 1).  $\tilde{p} > D_p$   
or  $\tilde{\theta} > D_{\theta}$

since the last data storage, indicating an event has occurred

- 2). The sensor must be functioning properly. That is, if there were too many spurious first differences greater than B (i.e. number of bad spikes,  $j_p = J_p$ ) then that channel can not trigger a critical for F samples (typically 1 day).
- 3). At least 128 samples have been taken since the last command to record data.
- 4). The event is not too long. That is, the number of criticals, which initiate data recording from the present event, must be less than

the preset limit of  $G_p$  or  $G_\theta$  events. Separate events are operationally defined by the absence of a "critical" for at least  $E_p$  or  $E_\theta$  samples. Thus marginal intensity data at the end of one event will be assigned to that event.

- 5). The number of events associated with a particular parameter is not excessive. The number of criticals, which initiate storage of data, must be less than the number,  $H_p$  or  $H_\theta$ , selected for a particular experiment.

If all these conditions are met, the raw high frequency samples for all parameters are recorded on cassette tape.

#### HARDWARE DESCRIPTION

The seafloor instrument package shown in figure 12 is capable of taking measurements of bottom pressure, water temperature, current speed and direction for up to one year. This prototype package contains two separate electronics cases for recording either high or low frequency data in addition to temperature, pressure and current sensors, an acoustic diagnostic system and recovery equipment. The low frequency sampling unit (KELVIN) averages and records sensor output over a 7 1/2 minute sample period and controls the operation of the sensors as well as the acoustic diagnostic system. The conditional sampling unit (COSAP) contains a microprocessor with associated support electronics and can selectively record bursts of 128 one minute samples which are stored in memory when a physical "event" has occurred as discussed above.

The instrument package is attached to an aluminum frame which supports the components. For the purpose of discussion, these components will be separated into five groups: 1) KELVIN, 2) COSAP, 3) SENSORS, 4) ACOUSTIC DIAGNOSTICS AND 5) RECOVERY AND SUPPORT EQUIPMENT. It is important to note that each of

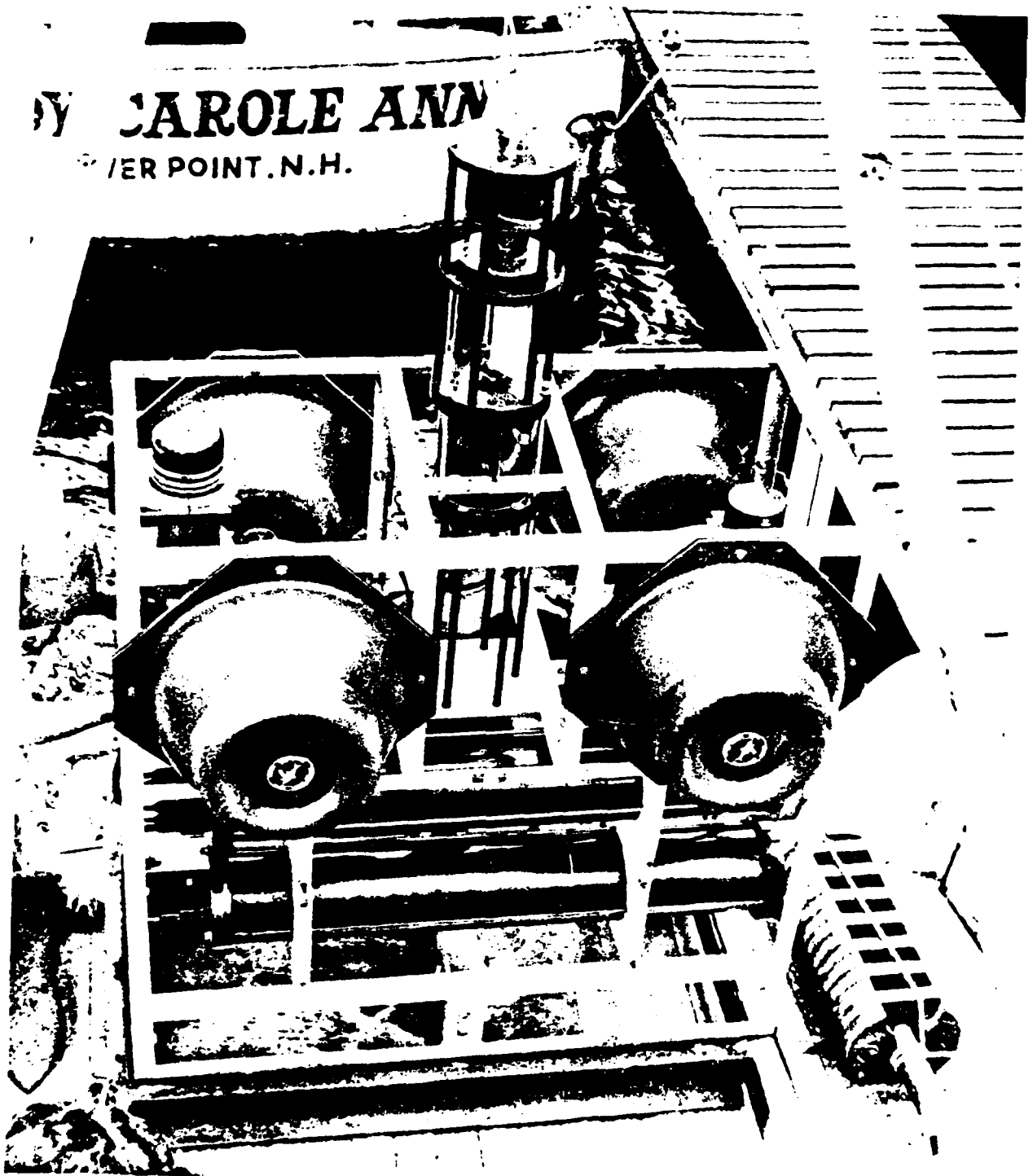


Figure 12. The conditional sampling instrument ready for deployment in the Gulf of Maine.

these components communicates with the others and cannot be considered as an isolated unit. A block diagram of the electronics is given in figure 13 for comparison with the following discussion.

#### KELVIN

The KELVIN electronics control the sampling of temperature, pressure and current sensors, record data at a specified time interval (nominally 7 1/2 min.) and provide acoustic diagnostics. This electronics package consists of a number of multipurpose plug in electronics boards produced by Sea Data Inc. and electronics designed and constructed at UNH. The Sea Data sub-systems used include a clock card (XC-19), sensor control and counter cards (XP-35), a data counter card for the current velocity (DC-40) and a magnetic tape data recording system (610-3). Electronics designed by UNH include a vane control and general interface card (VC-30) and a control card for the acoustic pinger (PLC-10) which is discussed in the acoustic diagnostics section.

The XC-19 card contains a stable quartz crystal clock circuit with an output of 16384 Hz and a network of four divide-by counters to provide output frequencies including signals of 7 1/2 minute periods (KELVIN sample rate), 64 second periods (COSAP sample rate), 1 Hz (pinger diagnostics) and 8 Hz (current meter logic timing). The XC-19 also has a sample counter circuit which provides a sample number to be recorded with each data cycle.

The XP-35 cards convert frequency modulated signals from the pressure and temperature sensors to digital data by frequency counting techniques. A voltage regulator is provided for stable sensor power. The sensor signal is conditioned in a shaper circuit, gated and fed into a counter circuit. At each sample command, the counted data is loaded into shift registers and serially strobed to the tape recorder. Then the counter is reset for the next sample.

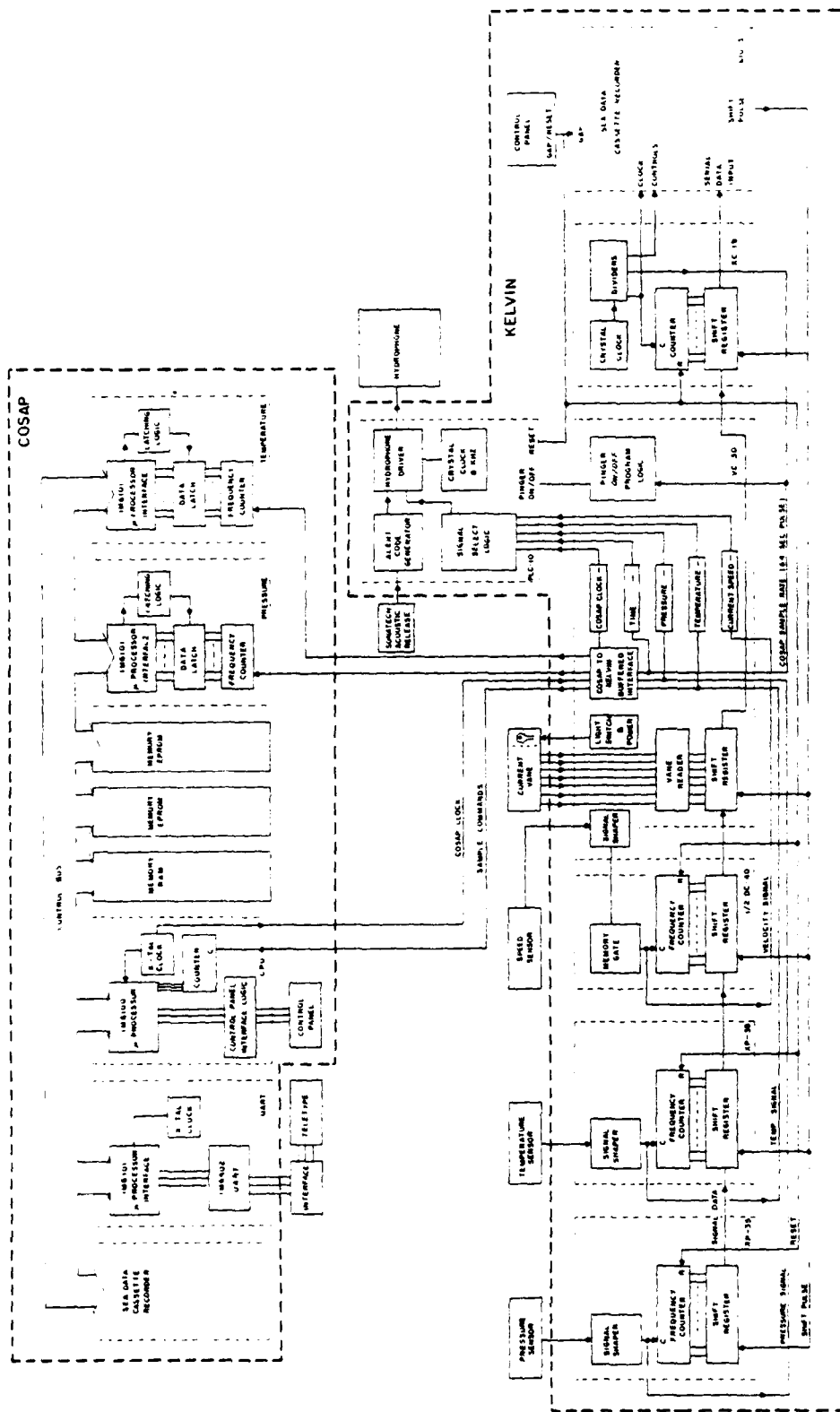


Figure 13. A detailed block diagram of the two systems (KELVIN and COSAP) shows the relationship and function of each electronic card.

The DC-40 card contains a pair of gating circuits and counters with shift registers, where the current velocity input is converted to digital data in a similar fashion to the XP-35.

The VC-30 is a multipurpose control/interface circuit board. The card contains binary counters which direct frequency signals to both the acoustic pinger and to COSAP. It contains timing logic which limits the acoustic pinger transmissions of diagnostics to the beginning and end of the deployment in order to conserve pinger power. The card also contains circuitry to interface the current meter rotor to the DC-40 card and to control the flow of data from the current meter vane. A combination of VC-30 and buffers contained in the COSAP unit is used to interface signals between KELVIN and COSAP.

The Sea Data tape recorder model 610-3 consists of a tape transport with three electronics control cards. The four-track recorder automatically records a record at each sample interval. Each record consists of a record gap, a preamble, a serial data stream and a parity code. The recorder has a capacity of 10 megabits on a standard 300 foot cassette tape.

#### COSAP

The conditional sampling electronics utilize a low power Intersil IM6100 microprocessor in association with 4096 words of memory, two sensor interfaces, an interface for a Sea Data cassette recorder and a universal asynchronous receiver and transmitter (UART) for interaction with a terminal. The IM6100 is a 12-bit microprocessor based on the architecture of the Digital Equipment Corporation PDP-8 computer. The instrument is configured so that a data and control bus is wired into the backplane and the circuit boards containing each of the system components are plugged into this bus. The pressure and temperature fm-signals are continuously sent from KELVIN to COSAP's interface cards, where

the signals are digitized. At each sample interval, the microprocessor takes these digital words, stores them in memory and processes the data as discussed in the previous section to determine if an event has occurred. If the event detection criteria are met, a record command is issued and the 256 memory locations (128 words for each sensor) plus a time word and a diagnostic word are sent to the recorder, where the data is stored permanently on magnetic tape.

The IM6100 is mounted on the CPU circuit board with a crystal clock, reset circuitry and some gating logic. The microprocessor has a 12-bit multiplexed data/address bus (Dx) with tristate ports for asynchronous data transfers. The timing control is generated within the IM6100 and is transmitted to the memory and interfaces by a eight line control bus. The time base is provided by an 800 kHz crystal clock. Reset switch circuitry provides a pulse to the IM6100 that clears the accumulator, loads  $7777_8$  into the program counter and halts the CPU. Then a run pulse, which starts the CPU, is issued. Also on the CPU card are logic gates for the MEMSEL and CPSEL outputs which are used for selecting memory transfers and control panel information.

The 10,000 octal words of memory (10,000 octal = 4096 words) in COSAP are contained on three separate circuit boards. One board contains the 0-1777 octal locations of RAM which is used for flag locations, data memory locations and other such volatile memory. Another board contains the 2000-5777 locations of Erasable Programmable Read Only Memory (EPROM), which contains the main conditional sampling program. EPROM is used where possible because of its lower power drain. The third board holds the 6000-7777 locations of EPROM which contains the system operating routines.

The physical structure of all memory boards is similar so that boards are interchangeable with the appropriate  $DX_0$  and  $DX_1$  code selection. All lines

have buffered inputs. A flip-flop for the  $DX_0$  and  $DX_1$  lines is clocked by the LXMAR line allowing for the proper timing to access the memory.

The fm-sensor signals are brought into the COSAP interface cards which create the digital words sent to the CPU through the IM6101 parallel interface element. The interface card contains a buffered signal input to a CMOS 12 bit counter. The outputs from the counter are connected to a data latch so the data can be strobed onto the DX bus at the appropriate times. The timing pulse is initiated by a command received by the IM6101 which transmits a DATA REQUEST pulse through FLAG 1. This pulse then disables the counter, loads the data onto the DX bus, resets the counter and enables the counter for the next sample. (In this prototype the timing sequence is imprecise as a result of the 100 pf capacitor on the counter disable line delaying the disable pulse. A small window now makes it possible for a count increment during the micro-processor's word sequence. This condition can result in small data errors. A few such errors have been observed and this situation has been corrected for subsequent deployments).

Each IM6101 interface has a different access code so each sensor can be accessed individually from the program. Also contained on the Interface card is an astable 3.3 kHz multivibrator used to simulate a sensor input during system testing.

For testing, programming, loading and diagnostics, it is necessary to access the microprocessor with a terminal. A separate interface port is used and a UART (IM6402) is connected to convert serial data for the terminal to parallel data for the microprocessor. A circuit board contains this interface hardware in addition to a 2.4576 MHz crystal clock and divider which are used to produce the proper baud rate for a particular terminal. Input buffers and driver transistors are also provided for compatible inputs and outputs. For a

detailed description of the operation of this UART as well as the other components in the microprocessor, reference should be made to the Intersil Data Books.

The final interface is required between COSAP and the tape recorder, a Sea Data Inc. microprocessor-compatible 10 megabit capacity cassette recorder Model 633M/6100. This is wired directly to the DX bus, and recording is performed under software control.

#### SENSORS

The temperature sensing element is a quartz crystal made by Hewlett Packard, driven by electronics designed by Integrated Circuit Instruments Inc. of San Diego, California. The whole sensor is packaged in a stainless steel case designed by Frank Snodgrass of Scripps Institution of Oceanography. The crystal is thermally isolated from the packaged electronics (see figure 14). The sensor has a nominal sensitivity of 1 m°C per Hz. This provides a least count resolution of 2.2  $\mu$ °C/count for KELVIN and is divided to 1/8 m°C/count for COSAP. KELVIN records 24 binary bits of data which correspond to an overflow every 37.28°C, while COSAP, with 12 bit resolution, overflows every 0.51°C.

The pressure sensor is a Paroscientific Digiquartz depth sensor model 8270 (see figure 14). It has a nominal sensitivity of 13 Hz per dbar. In KELVIN, this provides a least count resolution of  $0.17 \times 10^{-3}$  dbars (0.2 mm of equivalent sea water height, H<sub>2</sub>O). In COSAP, the least count resolution is 1.3 mm H<sub>2</sub>O. KELVIN records 24 bits of pressure data so overflows occur every 3024 m H<sub>2</sub>O. In COSAP with 12 bits of data, overflows occur every 5.33 m H<sub>2</sub>O.

The current meter is a Savonius rotor with a direction indicating vane. The rotor has two magnetic switches so one revolution, which corresponds to a

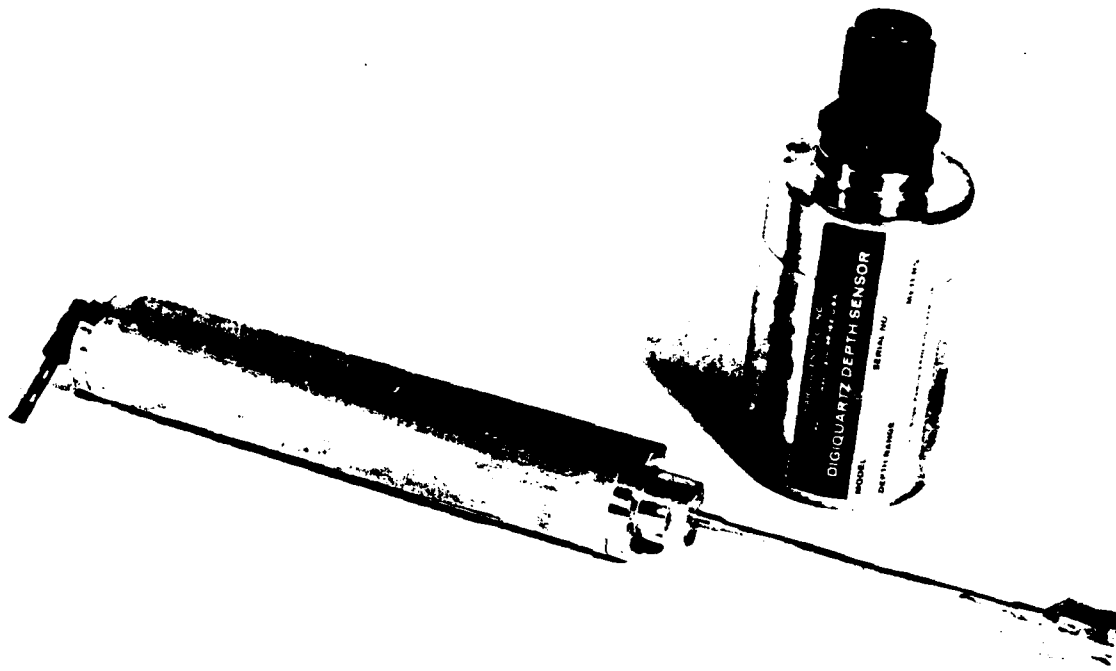


Figure 14. The Paroscientific pressure sensor (rear) and Hewlett-Packard temperature sensor (front) are shown.

water movement of about one meter, is identified by two pulses. For KELVIN, this gives a least count resolution of 0.0011 meters per second water velocity, with 16 bits of data storage an overflow would occur at a speed of 72.8 m/sec. The direction sensor contains a grey coded disc magnetically connected to the vane. A light is flashed above the grey-coded disc and seven fiber-optic light pipes positioned below the disc transmit the coded signal to a network of photo resistors, which convert the signal to a digital signal which in turn is accepted by KELVIN on the VC-30 card. This system can resolve flow direction changes of 2.8°. Since this instrument is stationary on the sea floor, there is no need for a compass signal input.

#### ACOUSTIC DIAGNOSTICS

The acoustic diagnostic system, which is used to check system operation on the sea floor, consists of a logic circuit board (PLC-10) to encode signals from the sensors and clocks, and an acoustic transponder with associated driver circuitry mounted in its own pressure housing. The acoustic pinger was manufactured by International Transducer Corporation and will produce an output of 7-8 kHz 200 watts (95 db rel 1 $\mu$  bar @ 1 yd) of acoustic energy. The PLC-10 contains switching logic which can sweep through 10 sensor or other frequency modulated signals and send an 8 kHz, 10 millisecond pulse to the pinger at each modulation of the sensor input. The sweeping sequence consists of 30 seconds for each input so that one sequence of all inputs takes five minutes. Timing from the VC-30 logic turns the system on for 8 1/2 minutes every 1/2 hour at the beginning and end of the deployment in order to conserve pinger power. An alert code generator is also contained in the PLC-10 which will override the diagnostic signals. Eight separate inputs are provided for interrupting the pinger system. Each input produces a different timed sequence of 10 millisecond

pulses. Presently only one input is used as an indicator that the Sonatech Acoustic Release has been activated. Since most signals are divided before being sent to the pinger, the resolution of the sensor signals is reduced but the system provides enough resolution to indicate the status of all sensors and clocks. This system is being expanded to include an FSK digital link which will transmit actual digital data from the microprocessor's memory to a surface receiving station.

#### RECOVERY AND SUPPORT EQUIPMENT

The instrument package is attached to an aluminum frame which supports the system components. The electronics canisters, sensors and backup timer are positioned in the lower section of the frame while the acoustic transponders, current meter, flashing light, radio and buoyancy spheres are positioned in the upper section. This allows for current measurements at 2 meters from the sea floor, visible recovery light and radio, and acoustic transmission with reduced structural interference while maintaining stability both on the sea floor and while floating on the surface. During a deployment and when on the bottom, the instrument rests on an iron anchor.

At the end of a deployment the instrument is released from its 160 kg anchor which is made from railroad rails welded to an angle iron cradle. The anchor is attached to the instrument frame by a dual-parallel release mechanism. A Sonatech model 310 acoustic release and a Horex 2500 series explosive bolt (environmentally protected by mounting in a steel sleeve with Devcon Flexane 80) are connected by a stainless steel linkage to an eye bolt on the anchor so that either mechanism may release the anchor. The exploding bolt is connected to a power source which can be activated by a quartz crystal CMOS timer. This timer

and 45 volt power source are contained in a separate aluminum pressure housing. The timer can be set to trigger the bolt at any one hour interval up to 10,000 hours and is accurate to better than one hour per year. The Sonatech release can be commanded from a hydrophone at the surface to release the anchor using a deck unit model S-1084. This unit is also used to locate the instrument on the sea floor since it has a transpond feature capable of measuring the distance between the bottom instrument and the ship. When the instrument is released, four Benthos 17" glass buoyant spheres provide a net buoyant force of 45 kg to bring the instrument package to the surface. Recovery is then aided by use of a CB transmitter and a flashing light manufactured by Ocean Applied Research.

#### FIELD TEST AND RESULTS

The conditional sampling scheme and prototype instrumentation described above were tested in 25m of water between 28 June and 5 July 1979 near Portsmouth, N.H. A summary of the high and low frequency data from that test are shown in figure 15. Due to a conservative selection of event criticals, the intensity for either temperature or pressure nearly always exceeded critical. As expected the pressure record is dominated by tides, while the tidal signal is less obvious in the speed and first half of the temperature record. The last half of the temperature record is dominated by an advection of horizontal temperature structure by tidal currents.

The upper set of records in figure 15 consist of values which were found by averaging 60 of the 64-second ( $64^S$ ) samples. This "box car" filtering is equivalent to the averaging performed by KELVIN, which counts the sensor frequency over the sample interval of 64 minutes ( $64^m$ ). A comparison of the  $64^S$  and the  $64^m$  data clearly show the differences between high and low frequency

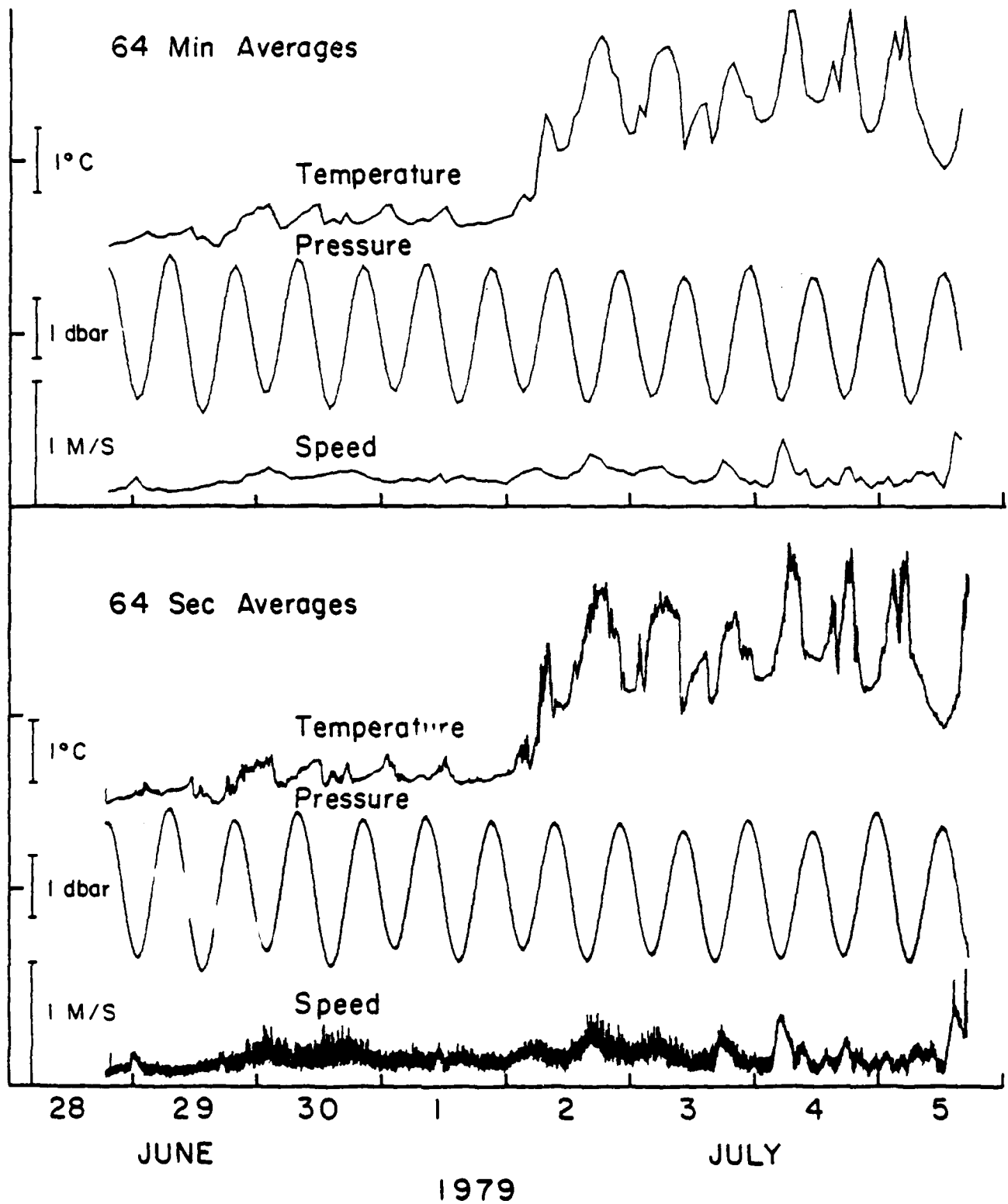


Figure 15. The 64 second averages of temperature, pressure and speed at 25m are shown at the bottom, and the 64 minute averages at the top.

sampling. The pressure records are most similar, and the speed least. Speed and temperature records contain high frequency fluctuations which give the lower set of signals their "character". High frequency fluctuations of temperatures on 2 July 79, when a warm front arrives, are unresolved in the averaged results.

The records of 64<sup>S</sup> data were used to recreate the pressure, temperature and speed intensity computations. The results of this computation and its intermediate results for the pressure record are shown in figure 16. Because the tides dominate, any high frequency pressure fluctuations are difficult to detect in the raw pressure record. The first difference filter prewhitens the record, which suppresses the tides, and amplifies the high frequency content. At this stage the tides are suppressed but are still the dominant energy containing frequency (see figure 8). The tide filter removes this tide, and leaves the high frequency variations. The intensity calculation shows what could be interpreted as two pressure events on 30 June and a single event near the end of the record on 5 July 1979.

A simulation of the conditional sampling computation for the temperature record is shown in figure 17. The first difference filter removes the low frequency part of a temperature signal which is distinctly different from the others. The only apparent tidal effects left at this stage are the "bursts" of fluctuations around low tide (for spectrum see figure 9). The intensity computation shows the onset of a "temperature event" on 2 July. The average intensity rises and remains higher after the start of the warm water intrusion. Again several events can be identified.

Although the speed record was not conditionally sampled during the actual deployment we simulated the conditional sampling as we did above for pressure and temperature. The results of this computation are shown in figure 18.

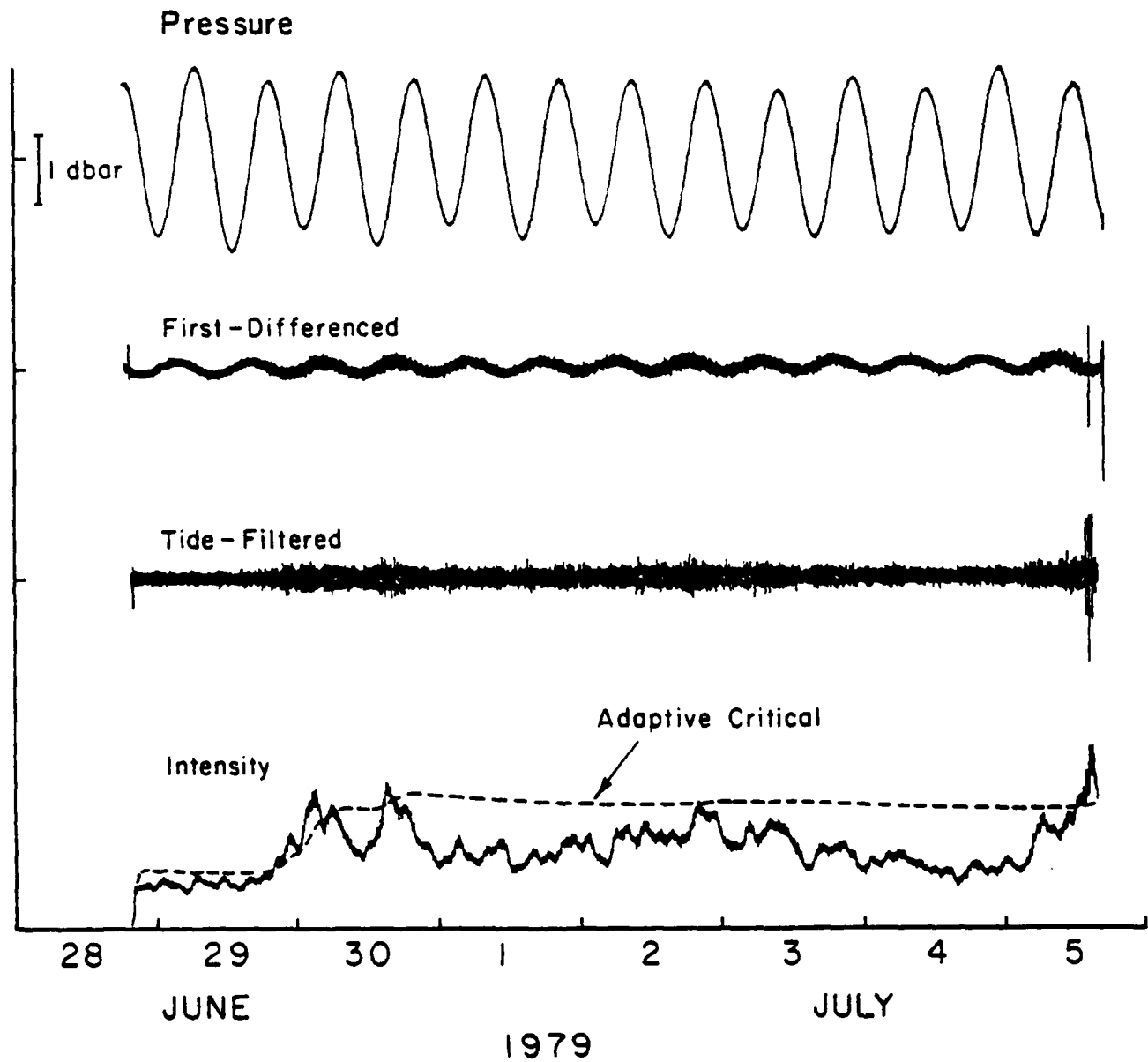


Figure 16. The conditional sampling process simulation on the computer. The pressure record shown in Figure 15 is at top, then the first difference record, tide-filtered record, and finally intensity at the bottom.

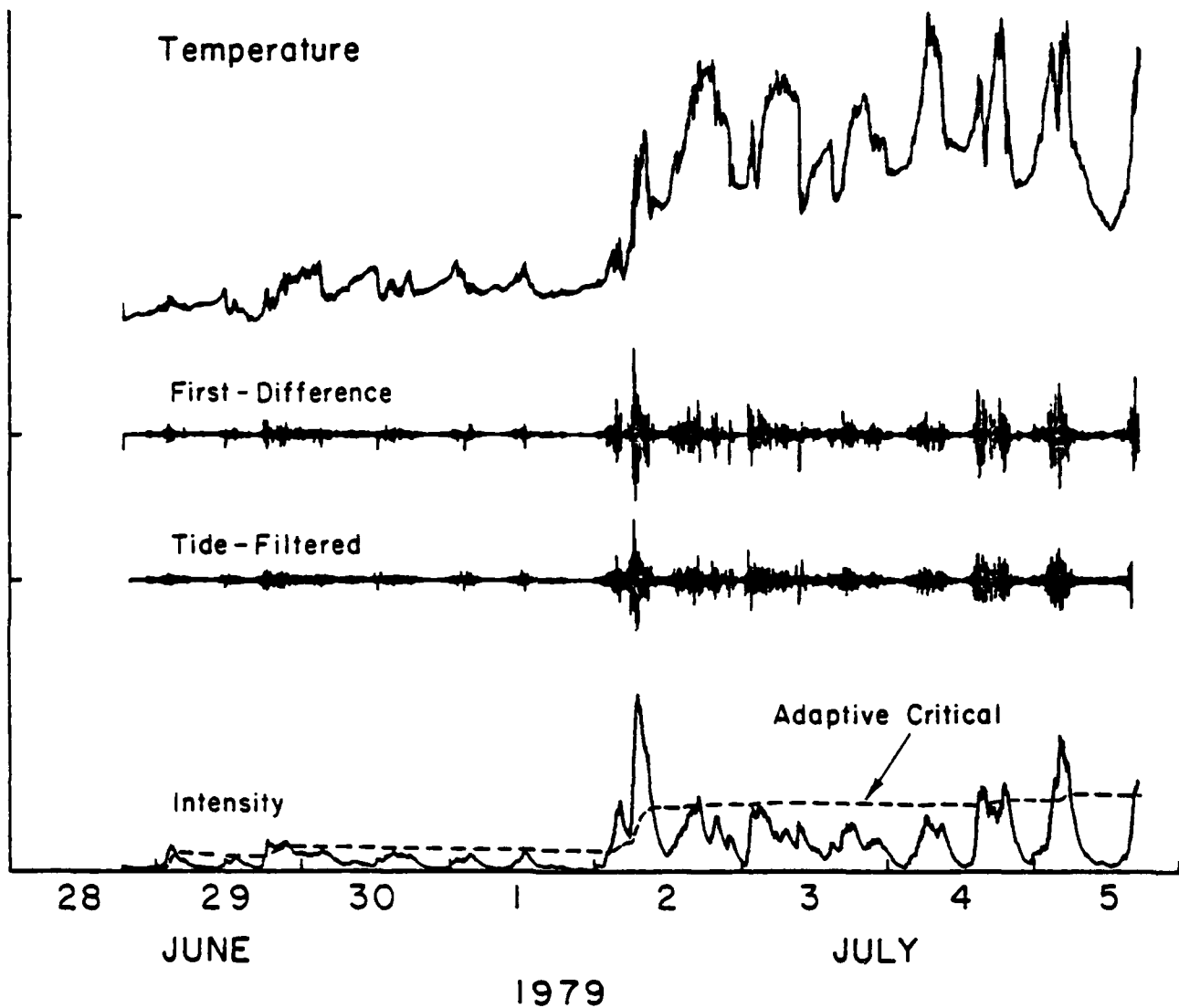


Figure 17. Similar to Figure 16 for temperature.

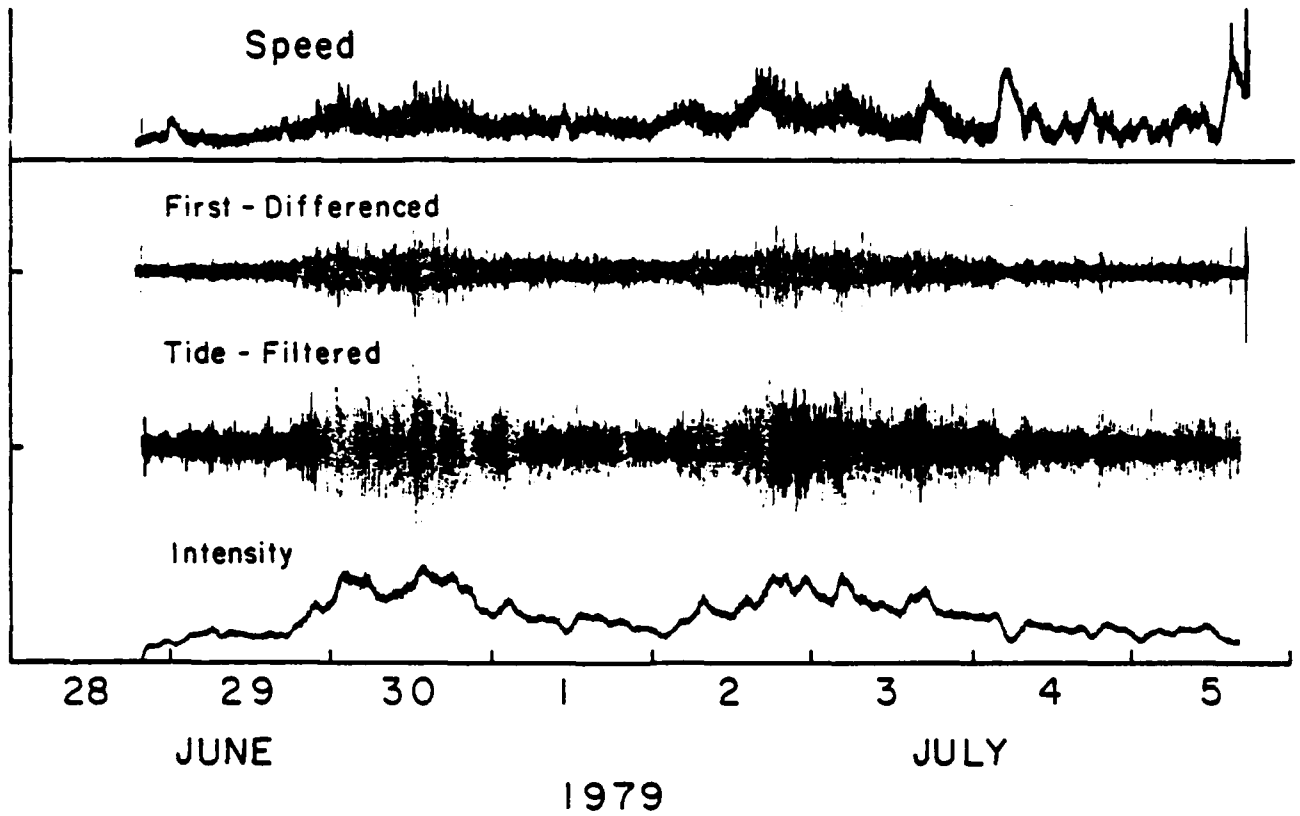


Figure 18. Similar to Figure 16 for speed.

Unexpectedly the raw speed record contains little tidal energy, which may be due to local topographic influence. Nevertheless, since current records usually have appreciable tidal energy, that first differenced record was tide-filtered and the intensity calculated.

For comparison, the intensities for pressure, temperature and speed are plotted in figure 19. The pressure and speed intensities are similar with both showing the double event on 30 June and event at 2-3 July. They differ in that the pressure intensity rises near the end where the speed does not. The temperature intensity record is distinctly different with no events indicated during 30 June or 2-3 July. On the other hand a major temperature event is indicated on 2, 4 and 5 July at times when there are no corresponding "pressure-speed events". Without speculating about the details it is clear that two different processes have left distinctly different dynamic signatures in our 64<sup>S</sup> records of pressure-speed and temperature.

The results of this test clearly indicate the problem of choosing the appropriate critical intensity levels for an environment with little prior knowledge. For longer such deployments we could fill our conditional sample tape with relatively less important events in the beginning and leave some more significant events unrecorded.

To avoid this problem or the alternate problem of recording no events if criticals are set too high, an adaptive sampling scheme has been devised. In this scheme we examine the intensity and determine an insitu value for the critical intensity, which is based on the statistics of the intensity itself. The following relation is used to determine adaptive critical intensity,  $D^a$ ;

$$D^a = \bar{X}_k + 2\sigma_k, \quad (22)$$

where the accumulated mean,  $\bar{X}_k$ , is defined by

$$\bar{X}_k = \frac{1}{k} \sum_{i=1}^k X_i ; \quad (23)$$

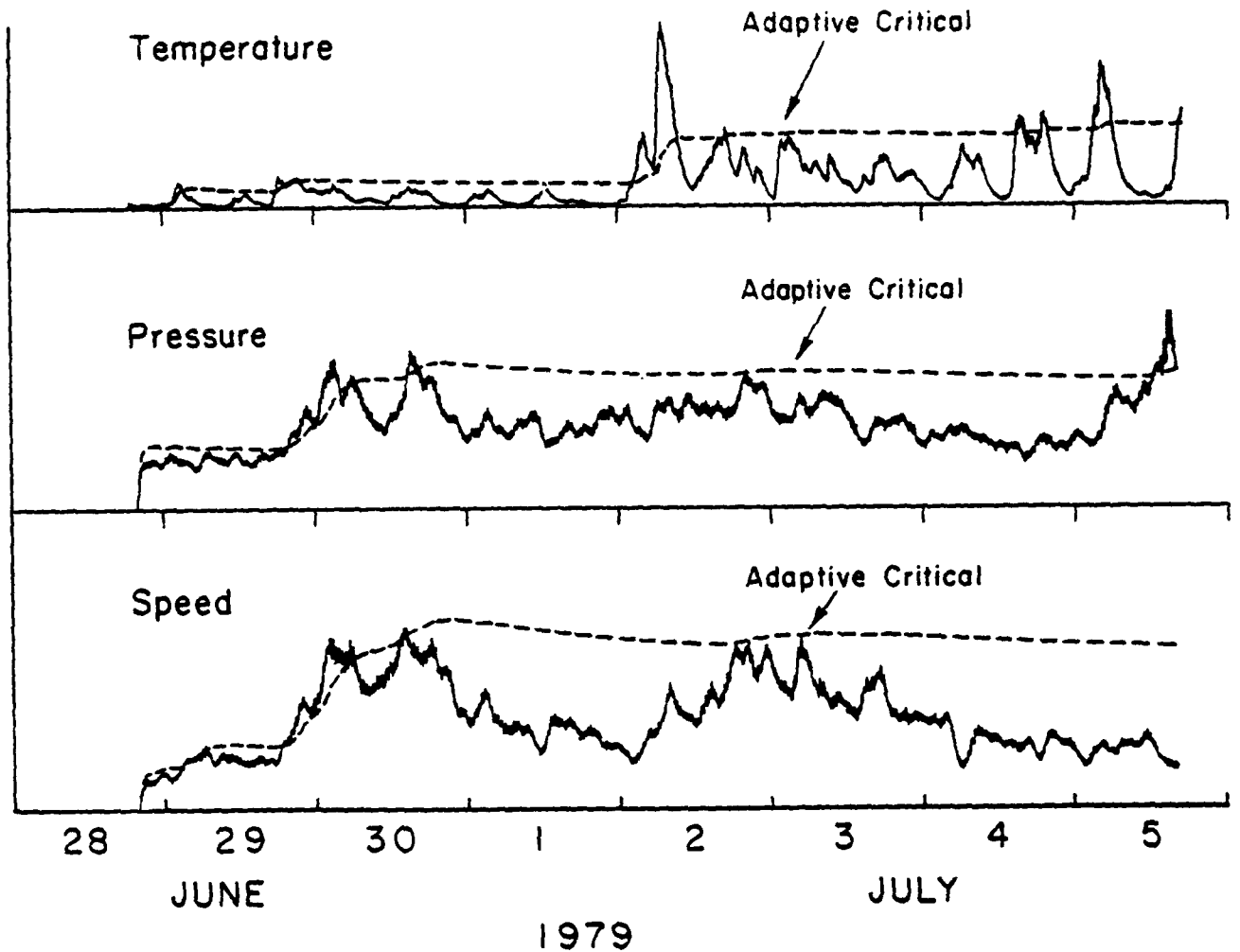


Figure 19. A summary plot of the three intensities is given with the adaptive criticals (dotted line) calculated according to equation 22.

and the standard deviation,  $\sigma_k$ , is defined by

$$\sigma_k^2 = \frac{1}{k} \sum_{i=1}^k [X_i - \bar{X}_k]^2 . \quad (24)$$

Thus both these statistics are based on all accumulated results from start of the experiment to the present term  $k$ . These adaptive criticals  $D_p^a$ ,  $D_\theta^a$  and  $D_s^a$  are plotted as the dotted lines on figure 19. They do a good job of identifying the principal events, even though the criticals are low and statistics uncertain at the start of the experiment. A limitation of this approach is demonstrated in the temperature computation. Since the statistics of the temperature record do change significantly after the 2 July event, tape is going to be wasted during the first part of the record when the statistics are poor. Nevertheless we feel that for exploratory experiments the use of an adaptive sampling scheme will be better than guessing constant critical levels.